Check for updates

physica status solidi (a)

REVIEW OPEN ACCESS

Detection Techniques for Polycyclic Aromatic Hydrocarbons and Their Metabolites: A Review

Martin Wolfgang Konrad[1] | Jeroen Vanoirbeek[2] | Patrick Wagner[1] | Irene Taurino[3,4,5]

[1]Soft Matter and Biophysics, Department of Physics and Astronomy, KU Leuven, Leuven, Belgium | [2]Environment and Health, Department of Public Health and Primary Care, KU Leuven, Leuven, Belgium | [3]Micro and Nano Systems (MNS), Department of Electrical Engineering, KU Leuven, Leuven, Belgium | [4]Semiconductor Physics, Department of Physics and Astronomy, KU Leuven, Leuven, Belgium | [5]Center for Biomolecular Nanotechnology, Istituto Italiano di Tecnologia, Arnesano, Italy

Correspondence: Patrick Wagner (patrickhermann.wagner@kuleuven.be)

Received: 15 June 2026 | **Revised:** 7 August 2026 | **Accepted:** 13 August 2026

Keywords: environmental analysis | functional interfaces | metabolite analysis | polycyclic aromatic hydrocarbons | sensors

ABSTRACT

Polycyclic aromatic hydrocarbons (PAHs) are a class of organic pollutants affecting the environment as well as individual health that has been linked to various diseases including cancer. Detection is focused on PAHs themselves for environmental analysis, and on urinary metabolites for human exposure assessment. Laboratory-based detection methodologies such as liquid or gas chromatography coupled with mass spectrometry have been established for more than 30 years and significantly improved over the years in terms of sensitivity and throughput. Outside of a laboratory environment, sensing close to the point-of-care could enable quick and simple analysis for routine testing, and various bio- and chemosensors utilizing different transducer designs have been developed to address this issue. This narrative review reports the state of the art in sensing PAHs and their metabolites, discussing laboratory-based techniques before focusing on techniques that promise to enable in-situ use at the point-of-care and in environmental settings.

1 | Introduction

Polycyclic aromatic hydrocarbons (PAHs) are a class of planar organic molecules composed of multiple fused aromatic rings with predominantly sp^2-hybridized carbon atoms and delocalized π-electron clouds. They are considered environmental pollutants, and environmental toxic thresholds have been regulated by governing bodies around the world [1–3]. PAHs originate from incomplete combustion of organic matter such as wood, tobacco, fossil fuel like coal, gasoline, and other petroleum-based products [4–6]. Exposure to PAHs is linked to a variety of health issues, including elevated cancer incidence rates, metabolic syndrome, damage to the cardiovascular system, and disruption of the endocrine system [7–12]. Commonly studied PAHs include pyrene, phenanthrene, benzo[*a*]pyrene (B[*a*]P), and naphthalene. Besides incidental exposure, e.g., from smoking or consuming barbecued foods, they are particularly concerning for individuals exposed to them in an occupational setting, such as firefighters, who are subject to elevated rates of bladder cancer [13], myeloma, and prostate cancer [14, 15]. As PAHs are lipophilic, they can easily enter the human body through the skin, via inhalation, and by ingestion [16]. Inside the human body, they are metabolized in the liver to a variety of different compounds, of which 1-hydroxypyrene (1OHP) is established as biomarker for exposure assessment due to its abundance in urine after PAH exposure [17–19]. Other urinary metabolites include 1-naphthol (1OHN), 2-naphthol (2OHN), and hydroxyfluorene [19–21]. The most relevant matrices for PAH analysis are aquatic samples from surface water bodies in the environmental context and urine samples in the medical context.

Figure 1, Panel a depicts eight PAHs that were determined to be particularly carcinogenic by European legislation [1]. Figure 1, Panel b illustrates the typical path of PAHs from formation to

This is an open access article under the terms of the Creative Commons Attribution License, which permits use, distribution and reproduction in any medium, provided the original work is properly cited.

© 2026 The Author(s). *physica status solidi (a)* applications and materials science published by Wiley-VCH GmbH.

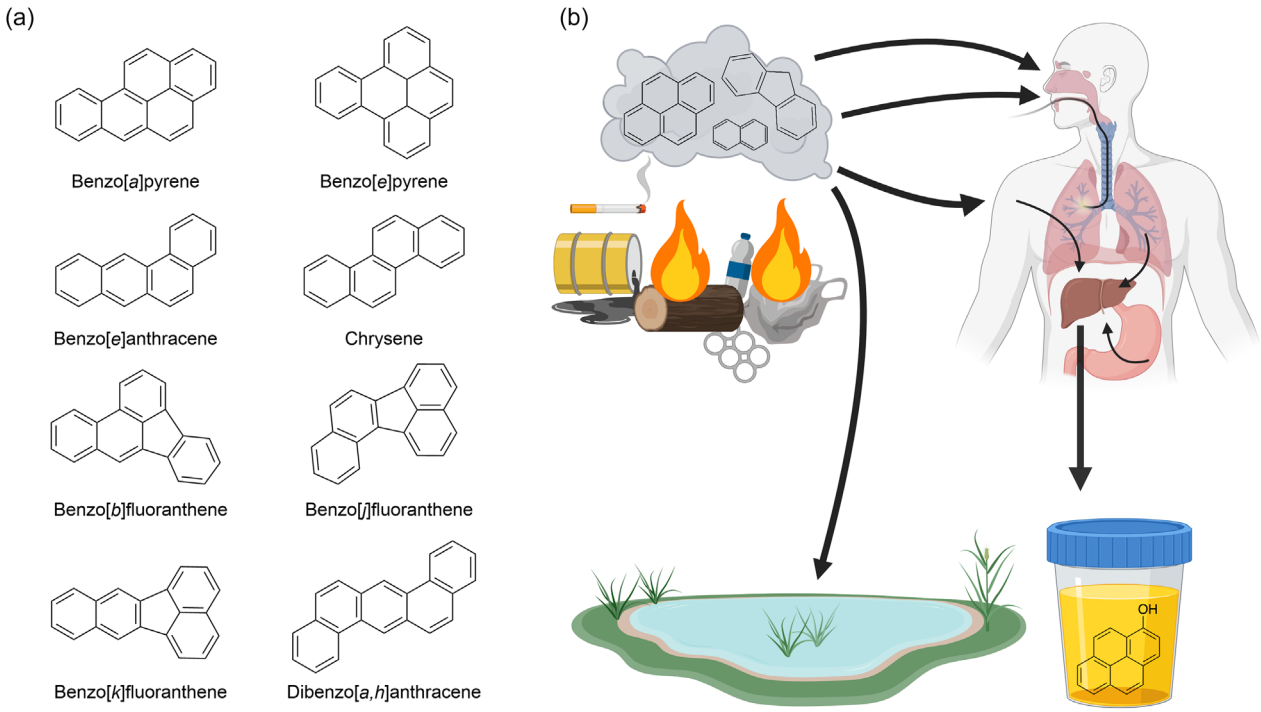

FIGURE 1 | Panel (a) Eight particularly relevant PAHs as defined by the EU directive on Registration, Evaluation, Authorization and Restriction of Chemicals (REACH) [1]. The conjoined aromatic rings of the molecules cause a delocalized π-electron cloud, lipophilicity, and high stability. Panel (b) The common pathways of PAH pollution, exposure, and metabolization. PAHs are formed by combustion of organic matter under oxygen-deficient conditions. They are commonly attached to particulate matter that also results from combustion process. By coming in contact with aquatic bodies, they cause environmental pollution. Upon skin contact, inhalation, or ingestion they enter the human body, where they get metabolized in the liver. Dihydrodiol epoxides, which are metabolic products of benzo[*a*]pyrene, are primarily responsible for the carcinogenic nature of PAH exposure. The urinary concentration of another metabolite, 1-hydroxypyrene, is commonly employed to assess total PAH exposure. Image created with biorender.com.

metabolization and excretion. Besides these eight PAHs, a set of 16 PAHs that are particularly relevant as environmental pollutants has been monitored for the last few decades [22–24]. Among different PAHs, B[*a*]P was found to be particularly relevant for the carcinogenic effects of PAH exposure [16, 25]. The mutagenicity of B[*a*]P is commonly attributed to the formation of a so-called Bay-region dihydrodiol epoxide from B[*a*]P during metabolization by the enzyme cytochrome P450 1A1 (also called CYP450 or CYP1A1) [26–29]. The formed dihydrodiol epoxide then reacts with DNA molecules, leading to faulty gene expression that, in turn, promotes cancer formation [29]. The metabolization mechanism is schematically depicted below in Figure 2. Monomethyl-substituted B[*a*]P has also been found to be genotoxic, but its genotoxicity is heavily dependent on the position of the methyl group, and the metabolic pathways responsible for forming strongly mutagenic compounds in humans have yet to be elucidated [28].

Effectively detecting the presence of PAHs in environmental samples, as well as the level of human exposure to them, is relevant from an environmental and health perspective [10, 30–32]. Laboratory-based techniques such as high-performance liquid chromatography followed by fluorescence detection (HPLC-FD) or gas chromatography coupled mass spectrometry (GC–MS) are considered the reference point for measuring PAH concentrations in samples directly and for assessing previous exposure

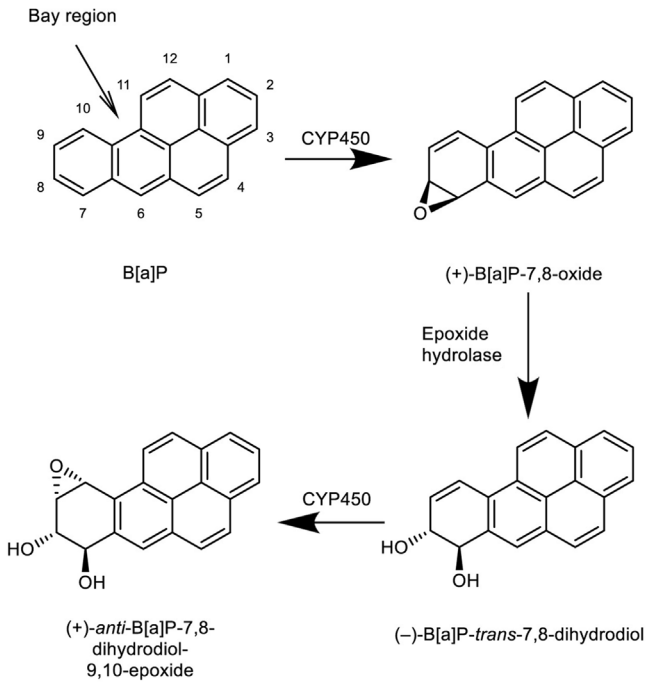

FIGURE 2 | Metabolic pathway of benzo[*a*]pyrene in the liver, leading to the formation of a dihydrodiol epoxide, which is capable of forming DNA adducts and thus promoting cancer formation. Adapted from [28] Copyright 2022, Elsevier.

18626319, 2026, 17, Downloaded from https://onlinelibrary.wiley.com/doi/10.1002/pssa.70497 by Martin Konrad - Ku Leuven , Wiley Online Library on [07/09/2026]. See the Terms and Conditions (https://onlinelibrary.wiley.com/terms-and-conditions) on Wiley Online Library for rules of use; OA articles are governed by the applicable Creative Commons License

by detecting the urinary concentrations of metabolites such as 1OHP [17, 18, 20, 33]. Chromatographic methods are required to isolate specific PAHs and metabolites from the sample matrix and detect them selectively thereafter. Detection by fluorescence is possible for most PAHs and their metabolites due to their fluorescence properties. While HPLC-FD and GC–MS are established and reliable techniques that can detect PAHs and their metabolites even in nanomolar concentrations, there are a number of general disadvantages when utilizing them for sensing: (I) They require a dedicated laboratory environment, (II) they need expensive equipment, (III) they rely on trained personnel, (IV) they require extensive sample processing, and (V) it takes multiple days between sample collection and results communication, preventing real-time detection [34]. In addition, the extensive use of organic solvents for extraction has raised concerns from a health and green chemistry perspective [35]. Despite recent advances to increase throughput and lower the time needed to process and measure samples [36], there has been extensive research into developing mobile sensors. Being portable, they promise to be operated easier, cheaper, faster, and closer to the point-of-care or the point-of-need while achieving satisfactory selectivity and sensitivity. A plethora of different sensing principles, molecular recognition elements, and combinations thereof have been reported.

This narrative review aims to provide an overview of the current state of the art in detecting PAHs and their metabolites. It will first discuss laboratory-based methodologies, describing recent developments that enable faster results, higher throughput, and novel detection mechanisms. Subsequently, we will move to surface-enhanced Raman spectroscopy (SERS)-based sensing, which is mostly laboratory-based but shows promise for miniaturization and field use in the medium term. After that, the focus will be on different techniques that already enable in-field use or hold promise for it in the near future, including fluorescence-based sensors, bioassays, and various electrochemical sensors, including graphene- and polymer-based ones. Various biological and biomimetic recognition elements will be discussed. Finally, there will be a short summary and outlook on future perspectives for developing mobile sensors for PAHs and their metabolites.

The reviewed publications were selected with the aim of providing readers with an overview of the reference methods in laboratory-based testing, recent developments in that field, and techniques that promise to enable point-of-care and point-of-need sensing of PAHs and PAH metabolites in the near future.

A list of used abbreviations is given in Table A1.

2 | Laboratory-Based PAH Detection and Quantification

2.1 | Established Techniques Based on HPLC and GC for Separation and MS and FD for Detection

Due to exceptionally low limits of detection (LOD) and established research methodologies, laboratory-based methodologies involving HPLC, GC, MS, FD, and combinations thereof remain the gold standard [37, 38], particularly for applying sensing in the context of environmental analysis [6] and biomarker discovery studies in environmental and occupational exposure [8–10, 39–41]. They are the reference to which novel and emerging sensing methods and devices are compared. The most commonly used method for detection of PAHs and their metabolites, such as 1OHP, is HPLC or GC coupled with FD or MS. The sample is typically processed to remove interfering compounds and enable selective and sensitive detection. First, particulate matter is removed via centrifugation or filtration when testing environmental samples. Since urinary samples are typically analyzed for the content of 1OHP, they are treated with the enzyme β-glucuronidase and incubated overnight [10, 17, 33, 36, 42, 43]. Enzymatic hydrolysis converts the target from its conjugated form, 1OHP glucuronide (1OHP-gluc), in which it is mostly present in urine, to free 1OHP, which is more easily sensed [18, 44]. 1OHP is also excreted as sulfate conjugate, albeit in a much lower concentration than 1OHP-gluc, so sulfatase enzymes are sometimes added for enzymatic proteolysis [18, 44]. The samples are then extracted using solid-phase extraction (SPE) to remove proteins and other interfering components of urine [36, 42] or extracted with methanol [43] before being inserted into the HPLC column for measurement. Using a methanol- or acetonitrile-based solvent for elution, PAHs and their metabolites are eluted from the column separately and detected specifically [18, 33]. For use in GC, PAHs and their metabolites need to be derivatized, e.g., methylsilanes prior to measurement [40, 43].

Recent advances focused on exploring different ways to detect analytes [45], optimizing FD [46], and increasing throughput [36] while maintaining a LOD in the sub-nanomolar range [18]. Utilizing FD, Chen et al. reported a novel method for detecting multiple PAHs simultaneously by using the inner filter effect, which is based on fluorescence quenching (FQ) caused by PAHs due to their conjugated aromatic nature [45]. This enables PAHs to absorb light with wavelengths in the ultraviolet (UV)/visible range, which overlaps with the emission range of many fluorophores, leading to PAHs causing quenching of the detected light [45]. By fingerprinting the absorption characteristics of fluorescence emitted at different wavelengths by various PAHs, an array-based sensing approach combined with pattern analysis was used to simultaneously detect multiple PAHs in a single sample. The authors report a LOD of 57 nM calculated from their calibration in spiked water and validated their sensor against HPLC using spiked soil and sludge samples containing PAHs at micromolar concentrations. However, the approach still requires extensive sample processing as the PAHs from environmental samples needed to be extracted via Soxhlet distillation, as well as benchtop equipment to achieve the required precision in emitting and detecting light at different wavelengths, confining it to laboratory use for the foreseeable future. Wang et al. also utilized optical detection and reported a novel multichannel deep UV (DUV)-induced fluorescence detector setup with improved detection limits in HPLC and a reduced size [46]. By constructing a three-dimensional (3D) detector setup with multiple excitation sources and collection paths and by incorporating excitation filters as reflectors for DUV, they increased the intensity of the excitation light. This enables higher efficiency since more energy is transmitted to the analytes, enabling stronger emissions at a given concentration and thus a higher sensitivity. Utilizing this and multiple channels for identifying the ideal parameters for

18626319, 2026, 17, Downloaded from https://onlinelibrary.wiley.com/doi/10.1002/pssa.70497 by Martin Konrad - Ku Leuven , Wiley Online Library on [07/09/2026]. See the Terms and Conditions (https://onlinelibrary.wiley.com/terms-and-conditions) on Wiley Online Library for rules of use; OA articles are governed by the applicable Creative Commons License

each analyte, they obtained detection limits as low as 20 pM for different PAHs after separating them using HPLC.

Building on the work reported in [10] and improving on established laboratory workflows, Frederiksen et al. reported a streamlined online SPE-LC-MS/MS method for simultaneous quantification of eight hydroxylated PAH metabolites in urine samples [36]. They addressed the bottleneck in throughput caused by manually handling and processing urinary samples and then focused on minimizing these steps to accelerate the overall analysis process. They built a setup utilizing an autosampler and a multiport valve to incorporate the extraction required after enzymatic proteolysis of the urine samples into the overall setup, reducing handling steps and making the procedure work in an uninterrupted manner. Compared to conventional solid-phase or liquid–liquid extraction procedures, their SPE configuration markedly accelerated processing, increasing laboratory capacity from approximately 50 samples per week to 100 samples within 2 h. As enzymatic proteolysis is still required for their technique, overnight incubation of samples for quantitative conversion of conjugated metabolites into their free form could not be avoided, leading to approximately 24 h of total duration for an individual sample analysis. Despite this, the method considerably improved the analysis capacity of an analytical laboratory, which in turn improves the utility of using laboratory-based analysis for routine testing in the occupational health context, as outlined by the authors of ref. [36]. The setup achieved a limit of quantification (LOQ) down to approximately 0.15 nM (for 1OHP) and exhibits intraday and interday variabilities of 2.4%–8.1% and 1.6%–6.5%, respectively, for the eight different metabolites they studied [36].

A different approach to minimize the pretreatment time for urine samples in HPLC was reported by Gao et al. by using electromembrane extraction [47]. In their work, the target analyte was enriched in an acceptor phase by extracting it from the sample using a polymer membrane assisted by applying an electrical field to improve the transfer of the target analyte from the sample phase into the acceptor phase. This also proved advantageous in minimizing matrix effects caused by the sample solution. An improved sensing performance in the subsequent LC/MS analysis could be achieved by optimizing the pH, the extraction voltage, the extraction time, and the chemical composition of acceptor and sample phase, achieving a LOD of 0.3 nM [47]. They still required enzymatic treatment of actual urine samples by incubating for 4 h at 37 °C.

2.2 | Coupling PAH Metabolization With Luciferase Expression in Genetically Modified Cells

Another approach is using genetically modified cells transfected with a reporter gene for luciferase (which generates light upon expression) to develop a sensor based on chemical activated luciferase gene expression (CALUX) and detecting the light response [48]. In this work, the reporter gene for luciferase is placed under the control of a receptor responsive to the target analyte: the CYP1A1 gene, which also controls the metabolization of B[a]P into mutagenic dihydrodiol epoxides [26, 28]. When the analyte binds to and activates this receptor, it induces luciferase expression, generating a measurable light signal proportional to receptor activation. A measurement was conducted by exposing the cultured cells to samples in growth medium, incubating, washing, lysing, and measuring luciferase intensity on a luminometer. Using B[a]P as model analyte and B[a]P equivalents calculated for other PAHs based on the half-maximal effective concentration of B[a]P, a LOD of 52 pM is reported. The reported CALUX bioassay was employed in a field study on PAH exposure of firefighters as well [49]. An overview of laboratory-based sensing methodologies is listed in Table 1.

2.3 | SERS

Raman spectroscopy is based on inelastic scattering of light upon illuminating molecules, where changes to the vibrational modes of the molecules lead to energy shifts in the scattered light, which

TABLE 1 | Overview of selected laboratory-based methodologies including SERS for PAH and PAH-metabolite detection.

Methodology	Target	LOD, nM	Notes	References
HPLC-MS	1OHP	0.5	Established benchmark method for 1OHP detection	[18]
HPLC-FD with automated extraction	Multiple hydroxylated PAHs and phenanthrenes	<0.15	Increased throughput, LOQ = 0.15 nM	[36]
Fluorescence quenching of array of fluorophores	PAHs	57	Validated with spiked sludge and soil samples	[45]
HPLC-MS with electromembrane extraction	Multiple hydroxylated PAHs	0.3	Electromembrane extraction for analyte preconcentration	[47]
Luminescence in CALUX bioassay	B[a]P	0.052	Not specific among high molecular-mass PAHs	[48]
Ag/GO-mercaptane/Au NP sandwich SERS	Pyrene	10	Sandwich construction for trapping analytes	[50]
Au/PIL nanobowl/Au NP SERS	Pyrene, anthracene, phenanthrene, B[a]P	0.6	Analytes trapped in nanobowls	[51]

18626319, 2026, 17, Downloaded from https://onlinelibrary.wiley.com/doi/10.1002/pssa.70497 by Martin Konrad - Ku Leuven , Wiley Online Library on [07/09/2026]. See the Terms and Conditions (https://onlinelibrary.wiley.com/terms-and-conditions) on Wiley Online Library for rules of use; OA articles are governed by the applicable Creative Commons License

are detected. The wavenumber and intensity of these shifts can be used for qualitative and quantitative analyses, respectively. In SERS, the target analytes are adsorbed on a nanostructured metallic surface, causing localized surface plasmon-induced enhancement of the electromagnetic field, leading to higher intensity of the Raman shifts and thus, more sensitive detection [52]. For SERS to be effective, the incident light needs to interact strongly with the metal nanostructures on the surface to create a so-called "hot spot", where the adsorbed target molecule has to be immobilized within a few nanometers of the surface [50]. SERS can be used to detect compounds down to the nanomolar range and has been employed for the detection of PAHs as well [11, 50, 51]. A schematic illustration of the use of SERS for PAH sensing is depicted in Figure 3.

The main issue of using SERS for PAH detection is the low affinity between PAHs and metallic surfaces, so extensive surface functionalization is required to entrap the target analyte in the hot spot [53]. One way of creating hot spots for trapping PAHs is binding them via a mediating layer that can interact with PAHs, e.g., graphene due to its completely delocalized π-electron system [53, 54]. Building on this, Wang et al. developed a self-assembled sandwich structure consisting of (from bottom to top) silver (Ag) nanowires, graphene oxide (GO) for improved interaction with PAHs via $\pi-\pi$ stacking, mercaptans to enable thiol bonds for improved PAH trapping by hydrophobic interaction, and to enable immobilization of gold (Au) nanoparticles on top for a larger effect on the Raman shift [50]. They proposed that this metal–insulator–metal sandwich improved detection by trapping both surface plasmons and PAHs within the dielectric layer for intimate interaction and thus sensitive detection and linked the adsorption capacity of the SERS substrate to the intensity of the Raman signal and thus, to the sensitivity. Pyrene was identified by a characteristic SERS peak at 592 cm^{-1}, achieving a LOD of 10 nM for pyrene, anthracene, and phenanthrene in filtered and spiked river water [50].

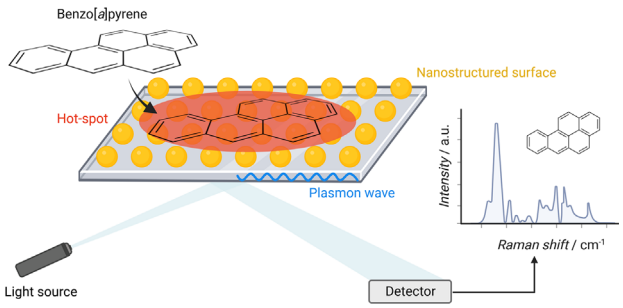

FIGURE 3 | Schematic depiction of SERS used for PAH detection. The target molecule, e.g., B[a]P, gets immobilized in the hotspot on a nanostructured surface with a suitable functionalization that enables binding via, e.g., $\pi-\pi$ stacking. The molecule needs to be located within a few nanometers of the surface for SERS to occur. Upon illumination with a laser, the analyte exhibits Raman scattering with characteristic Raman shifts arising from molecular vibrational modes. The signals are significantly amplified by surface plasmon resonances that occur at the nanostructured surface. The resulting Raman spectrum is used for molecular fingerprinting, and the intensity of the shifts can be correlated with analyte concentrations for quantification. Image created with biorender.com.

The authors improved their setup further by using bowl-shaped nanocavities that were filled with a poly-ionic liquid (PIL) before decorating the surface with Au nanoparticles [51]. As the PIL exhibited a very high affinity for PAHs, they could achieve a stronger signal intensity and more efficient entrapment via $\pi-\pi$ stacking and hydrophobic bonds between the PIL and the PAHs, leading to a sub-nanomolar LOD for multiple PAHs. Utilizing machine learning for fingerprinting, the SERS response of different structurally dissimilar PAHs, the individual PAHs could be differentiated from one another in spiked water samples. The authors report limitations as the model struggles to differentiate peaks corresponding to structurally similar analytes, which is even more pronounced in samples containing a large volume of organic matter—as is expected in, e.g., polluted river water. Despite this, the paper illustrates that selective and sensitive detection of PAHs in a laboratory context can be achieved without extensive analyte separation by utilizing complex 3D architectures and advanced signal processing techniques.

3 | Portable Sensing Technologies

Despite advances in laboratory-based detection of PAHs, there is considerable research interest in sensors operated locally without centralized laboratory infrastructure. Portable sensing technologies enable faster assessment of the degree of pollution and exposure, respectively, as the delay caused by transportation, processing, and results communication after sample collection is eliminated. In addition, accessible and affordable testing in the field and close to the point-of-care enables routine testing for early recognition and intervention in case of excess PAH exposure or pollution. Multiple types of recognition elements can be employed in portable sensors.

3.1 | Biological Recognition Elements

Biosensors in the strict sense are built on biological recognition elements, such as antibodies (AB), enzymes, cells, aptamers, or DNA fragments. They generally exhibit very high specificity due to, e.g., antibody–antigen (AB–AG) interactions. In an early approach, Wei et al. reported the development of a biosensor based on monoclonal ABs immobilized on silane-modified indium tin oxide (ITO) [55]. Target PAHs were labeled using a ruthenium tris(bipyridine)-pyrenebutyric acid conjugate as redox tracer, and an oxalate-containing electrolyte was used for amplifying the redox signal by acting as electron donor [55]. The use of these so-called labels is often required to form a suitable binding site at the target PAH, which enables competitive binding based on AB–AG interaction between the labeled PAHs and the immobilized ABs. Upon binding, a lower peak current is measured in a cyclic voltammogram, and the decrease could be linked to the PAH concentration, enabling sensor use. Achieving an LOD of 9.5 nM for B[a]P, the approach still relied heavily on modifying the target analytes in the process.

Ball et al. reported an enzyme-linked immunosorbent assay (ELISA) to detect urinary 1OHP-gluc [56]. Based on the ELISA concept, they developed a lateral flow assay for in-field detection. The detection element, a monoclonal AB, was bound to Au

18626319, 2026, 17, Downloaded from https://onlinelibrary.wiley.com/doi/10.1002/pssa.70497 by Martin Konrad - Ku Leuven , Wiley Online Library on [07/09/2026]. See the Terms and Conditions (https://onlinelibrary.wiley.com/terms-and-conditions) on Wiley Online Library for rules of use; OA articles are governed by the applicable Creative Commons License

nanoparticles and stored in the so-called "conjugate pad", which is a site along the flow direction that the sample passes. There, the sample can bind to this primary AB, which is linked to the previously mentioned Au nanoparticles. A secondary AB that can selectively bind to the primary one to form a sandwich assay is immobilized at the test line further down the lateral flow channel. For use, the urine sample is mixed with the assay buffer and a controlled volume deposited onto the conjugate pad. There, 1OHP-gluc binds to the first AB and is carried along the flow channel over an incubation period of 30 min. The ABs bind at the test line, and the resulting accumulation of Au nanoparticles leads to the formation of a red line, indicating a positive test [56]. A control line that should become visible regardless of the 1OHP-gluc content is located after the test line to validate the test procedure. The evaluation of the test is done using a smartphone camera and app. When using the lateral flow kit for qualitative (1/0) assessment only, the authors suggest a cutoff point of 21 nM for accurately detecting the presence of 1OHP-gluc in real urine samples. The authors report a link between the intensity of the test line color at a wavelength of 450 nm and the analyte concentration for the underlying ELISA setup, achieving a LOD of 21 pM calculated as three times the standard deviations of a blank sample measured in a laboratory setting. The test could successfully differentiate between 1OHP-gluc and competitors like pyrene, 1OHN glucuronide, and 1OHP.

Building on this, a sensor utilizing a competitive immunoassay as recognition element for electrochemical detection of 1OHP-gluc from urine was reported [57]. The sensor consists of hapten-bovine serum albumin (BSA) conjugates immobilized on the working electrode of a 3D-printed sensor in a three-electrode setup. A buffer solution containing a known concentration of sheep anti-1OHP-gluc ABs is mixed with a urine sample containing 1OHP-gluc, which binds with the polyclonal ABs in solution. The solution is then dropped onto the sensor surface, where unbound ABs bind to the hapten-BSA conjugates, while ABs attached to 1OHP-gluc cannot bind to the conjugates. A solution containing donkey antisheep IgG labeled with horseradish peroxidase (HRP) was added and binds to the immobilized ABs. Upon adding a solution containing hydrogen peroxide and thionine acetate, HRP acts as catalyst for the reduction of hydrogen peroxide to water and the subsequent oxidation of thionine acetate. At the electrode, the oxidized thionine is reduced again, which generates a current drop that is detected using differential pulse voltammetry (DPV). The measured peak current is inversely proportional to the logarithm of the 1OHP-gluc concentration in the urine sample [57]. The principle is depicted in Figure 4. An LOD of 250 pM is reported, with an analyte recovery of 95%–105% from spiked human urine. Selectivity is implied by the use of a specific AB but was not explicitly tested for using competing compounds.

Relying on bacteria and the enzyme β-galactosidase, Cho et al. reported a colorimetric biosensor based on *Escherichia coli* (*E. coli*) bacteria for detecting PAHs in aquatic media [58]. They genetically modified *E. coli* to carry a gene encoding a protein for naphthalene degradation and coupled their expression (the protein synthesis) with production of chlorophenol red-β-galactopyranoside (CPRG). Detection was then conducted by adding β-galactosidase. In the presence of naphthalene, the bacteria produce the enzyme for its degradation, thereby also

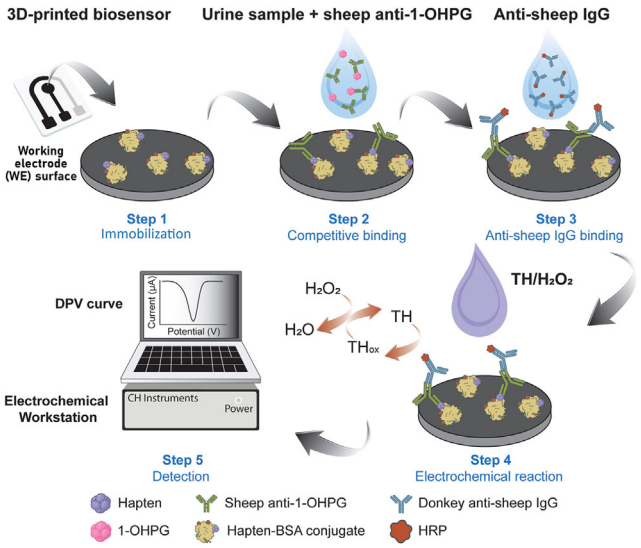

FIGURE 4 | Schematic depiction of a competitive immunoassay used as recognition element in an electrochemical sensor for 1-hydroxypyrene glucuronide. Reproduced with permission and adapted from [57] Copyright 2026, Elsevier.

producing CPRG, which is then in turn hydrolyzed by β-galactosidase. As hydrolyzed CPRG exhibits a bright red color, the change in concentration is reflected in a change in color, which can be detected by the naked eye [58]. The reported LOD for liquid samples in the micromolar range make it mostly suitable for heavily polluted water bodies. It should be noted that the sensor exhibited a lower LOD for gaseous samples, suggesting that it could be used in conjunction with a portable evaporator for rapid assessment of naphthalene presence. An overview of the reviewed sensors using biological recognition elements is listed in Table 2.

3.2 | Metal–Organic Frameworks (MOFs)

MOFs are a technology that received increasing attention in recent years, which is evidenced by the fact that their inventors Kitagawa, Robson, and Yaghi were awarded the Nobel prize for Chemistry in 2025 for their work [59]. MOFs are ordered molecular structures composed of metal ions or complexes that are connected via organic linker molecules [60]. They exhibit extremely high porosity and a correspondingly large internal surface area, which makes them ideally suited for catalytic and sensing applications [60–63]. Their properties can be easily tuned by varying the metal ions and the size and type of the linker molecule, enabling their use in a variety of different sensing applications [60, 63–65]. They were applied for sensing PAHs and their metabolites [61, 66, 67] based on their fluorescent properties, as well as for electrochemical detection [68–70]. MOFs themselves can also exhibit fluorescent properties, originating from resonance energy transfer, metal-to-ligand charge transfer, and ligand-to-metal charge transfer as well as from interactions with their guest molecules [71]. A schematic depiction of the MOF structure and its interaction with B[*a*]P is shown in Figure 5. Typical metal ions used in MOFs are transition metals or lanthanides, and common linkers include carboxylates, amines, and phosphates [60].

18626319, 2026, 17, Downloaded from https://onlinelibrary.wiley.com/doi/10.1002/pssa.70497 by Martin Konrad - Ku Leuven , Wiley Online Library on [07/09/2026]. See the Terms and Conditions (https://onlinelibrary.wiley.com/terms-and-conditions) on Wiley Online Library for rules of use; OA articles are governed by the applicable Creative Commons License

TABLE 2 | Overview of PAH sensors utilizing biological recognition elements.

Recognition element	Target	LOD, nM	Notes	References
Monoclonal antibody	B[*a*]P	9.5	Extensive sample processing	[55]
Monoclonal antibody	1OHP-gluc	21	LOD reported for lateral flow assay; tested for competing analytes	[56]
Polyclonal antibody	1OHP-gluc	0.25	Competitive assay; did not test for competing analytes	[57]
Enzyme-based colorimetric sensing	Naphthalene	>1000	Genetically modified *E. coli*	[58]

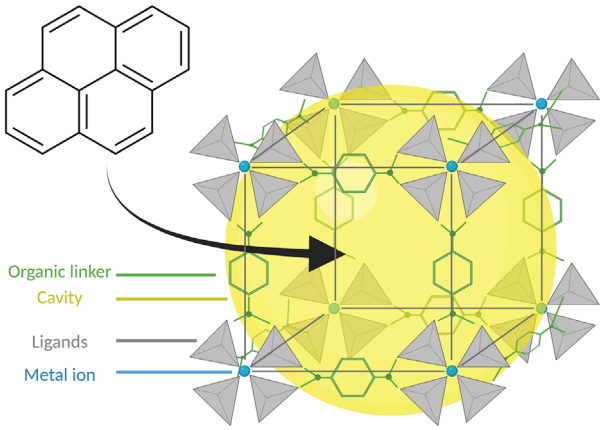

FIGURE 5 | Schematic depiction of a metal–organic framework and its interaction with B[*a*]P. The properties of MOFs heavily depend on the type of metal ions and the size and type of the linker molecule Image created with biorender.com and adapted from [72] Copyright 2014, Springer.

3.2.1 | *MOFs for Optical Detection*

Most MOFs exhibit fluorescent or luminescent properties, which can be utilized for sensing. Upon excitation with light of particular wavelengths, electrons in the MOF are elevated to higher energy states with the same spin multiplicity as that of the incident light, from where they slowly return to lower energy levels. This causes the absorbed energy to be slowly released as light with a wavelength corresponding to the energy difference [71]. Most MOF-based sensors operate on the principle of luminescence or FQ, where the inherent fluorescence or luminescence gets disrupted by the target analyte. Upon a target molecule entering the framework and interacting with the MOF (e.g., due to hydrophobic interactions or π-interactions), the emission is disrupted since the interaction between MOF and target enables the energy of the excited electrons to be transmitted towards the target via photoinduced electron transfer. This causes a reduction in the intensity of the emitted light at a specific wavelength, depending on the MOF used. This intensity reduction is proportional to the concentration of target analytes. In some cases, the energy transfer can also cause an increased intensity of emitted light at a different wavelength. By measuring the intensity changes at multiple wavelengths and calibrating for the change in ratio, a so-called ratiometric sensor can be designed. The sensing principle and calibration for a ratiometric luminescence sensor are depicted in Figure 6.

Various MOFs have been reported for sensing 1OHP, which show a detectable interaction with MOFs based on lanthanide group metals. Among them, europium (Eu^{3+}) ions were found to exhibit the best overall performance for 1OHP sensing [61, 73–76]. When sensing 1OHP at the point-of-care, the sample matrix is usually urine. Accordingly, the interference of other urine compounds like various ions and particularly uric acid is highly relevant [66, 67].

In an early publication on Eu^{3+}-centered MOFs for 1OHP detection, the authors used an UV lamp to excite the framework. Quenching in the presence of 1OHP was attributed to the overlap between the absorbance spectrum of 1OHP and the ligands, enabling an effective energy transfer from 1OHP to the ligands and from there to Eu^{3+} [61]. A LOD of 3.2 nM, little interference from ions and uric acid, and stability in a pH range of 4.5–8 are reported [61]. The authors also deposited the MOF onto a paper-strip to enable a quick qualitative assessment of 1OHP exposure by dipping it into urine samples and subsequently assessing the color of the dried paper strip under a UV lamp.

Yang et al. reported a stable FQ-based MOF sensor for 1OHP that was resistant to uric acid interference [73]. Subsequent publications from the same research group reported sensors with detection limits for urinary 1OHP at micromolar concentrations. The reported LOD is higher than the one reported in [61], but the sensor was found to be stable in a broader pH range of 2–14. However, these sensors were multisensors to both 1OHP and uric acid as both compounds caused strong FQ at the same wavelength for a given MOF, and the individual contributions of 1OHP and uric acid could not be distinguished [74, 75]. This is a common problem as uric acid is known to interfere with 1OHP detection—an issue that is particularly pronounced in urine samples due to the ubiquity of uric acid in urine. In a follow-up paper, the group addressed this issue by developing a zinc (Zn^{2+})-based MOF and using it to construct a ratiometric fluorescence sensor [77]. In a ratiometric sensor, the signal response is measured using the quenching ratio of two peaks at different wavelengths, which can enable differentiating between compounds that show similar quenching behavior at one wavelength but not at another. Eliminating the interfering effect, the sensor could accurately detect 1OHP at micromolar concentrations, albeit no explicit LOD is reported [77]. The technology shows promise for constructing a mobile sensor, albeit a lower LOD is necessary for real-life applications as urinary 1OHP is commonly found in nM and sub-nM concentrations [21, 78, 79].

18626319, 2026, 17, Downloaded from https://onlinelibrary.wiley.com/doi/10.1002/pssa.70497 by Martin Konrad - Ku Leuven , Wiley Online Library on [07/09/2026]. See the Terms and Conditions (https://onlinelibrary.wiley.com/terms-and-conditions) on Wiley Online Library for rules of use; OA articles are governed by the applicable Creative Commons License

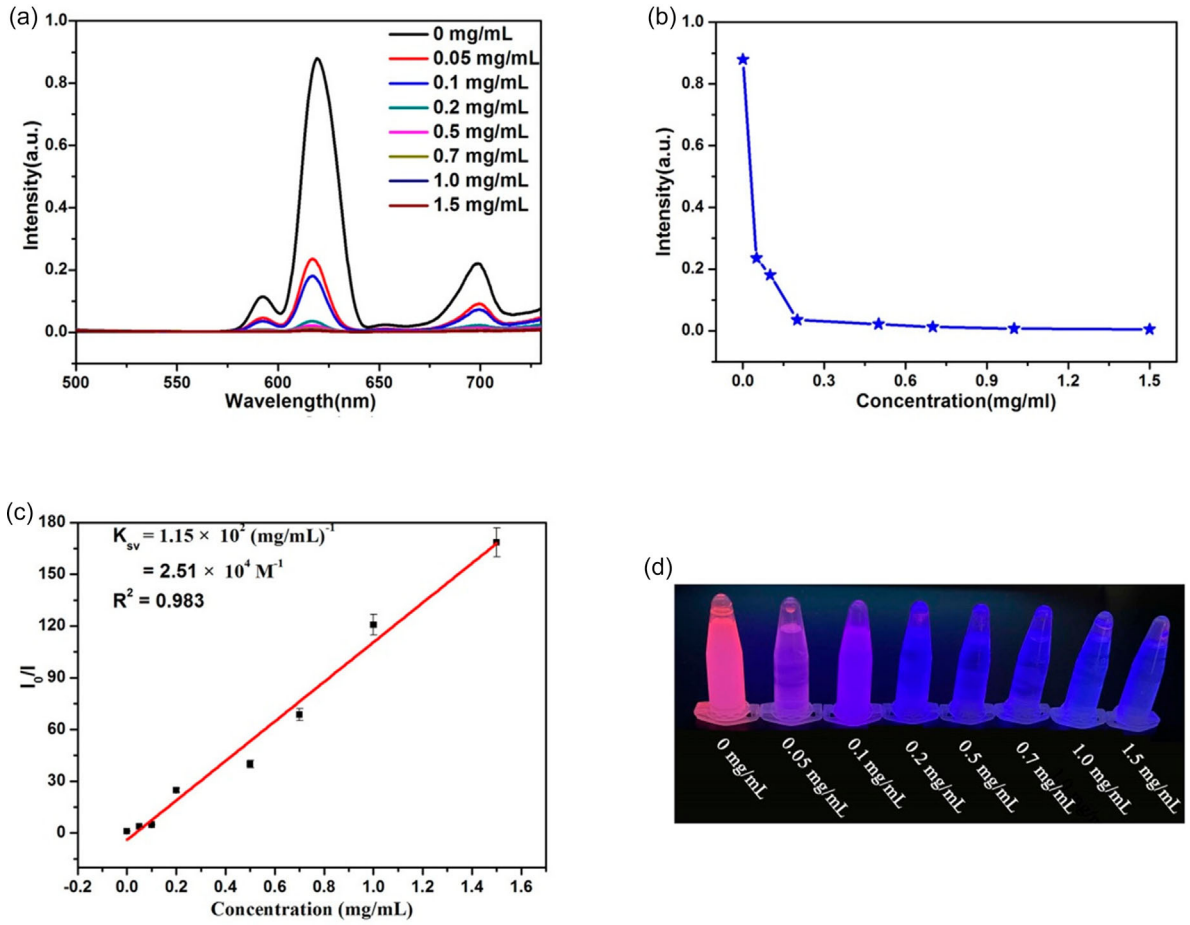

FIGURE 6 | Working principle of a ratiometric luminescence sensor for 1OHP utilizing europium-based MOF. After excitation at 310 nm, the intensity of the light emitted by the MOF complex at 618 nm is reduced by the presence of 1OHP (a) as a function of the 1OHP concentration (b), so the relative change is used for calibration (c). Solutions containing different concentrations of 1OHP also exhibit different colors under radiation of light with 365 nm wavelength (d). Reproduced with permission from [73] Copyright 2021, American Chemical Society.

Related to this, a ratiometric Eu^{3+}-based MOF sensor for 1OHP and copper (Cu^{2+}) was reported that achieved a LOD of 19 nM for 1OHP in water [80] but could not distinguish between the responses to 1OHP and Cu^{2+}.

Recently, lanthanide-centered MOFs based on FQ that did not exhibit interference by uric acid were reported. A study investigating multiple lanthanides for use with pentiptycene ligands also reported FQ-based sensors that could detect 1OHP without interference by uric acid and other common compounds, with Eu-based MOFs showing the best performance, but the sensing capabilities were only investigated at concentrations as low as 230 μM [76]. One publication also reported the development of Eu^{3+}-centered MOFs with insignificant interference by uric acid, good shelf stability, a LOD of 1.1 μM 1OHP in urine, and the sensor also responded to tryptophan [66]. A sensor that responds to both 1OHP and tryptophan was also reported using a cadmium (Cd^{2+})-based MOF [67]. In a different publication by Liu et al., ratiometric sensors based on terbium (Tb^{3+}- and Eu^{3+})-centered MOFs were developed, achieving a LOD in urine of 0.6 μM for the Tb^{3+} MOF and 150 nM for Eu^{3+} MOF, respectively, with good recovery of 1OHP from real urine samples [81]. They also constructed a benchtop setup using light-emitting diodes for illumination and a smartphone camera for detecting the resulting red-green-blue (RGB) components, which shows promise for point-of-care applications in the near future once the LOD can be sufficiently lowered.

3.2.2 | *MOFs for Electrochemical Sensing*

MOFs were also used for electrochemical sensing of 1OHP [68–70]. Then, the MOF needs to be immobilized on a conductive support such as carbon, graphene, or a derivative thereof. Based on a chromium (Cr^{3+})-centered MOF regulated by polyamidoamine dendrimers, an electrochemical sensor using DPV for detecting 1OHP was reported [70]. The MOF is employed as catalyst for the electrooxidation of 1OHP on graphene oxide. The proposed oxidation mechanism resulting in a quinone is depicted in Figure 7.

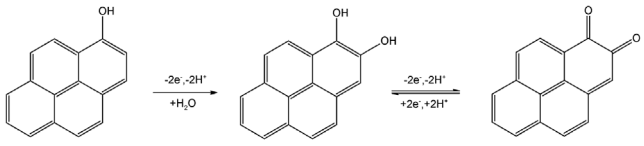

FIGURE 7 | Electrooxidation of 1OHP in aquatic media adding a hydroxy group and subsequently resulting in the formation of pyrene-1,2-quinone as reported in literature [82]. Reproduced with permission from [70] Copyright 2021, American Chemical Society.

18626319, 2026, 17, Downloaded from https://onlinelibrary.wiley.com/doi/10.1002/pssa.70497 by Martin Konrad - Ku Leuven , Wiley Online Library on [07/09/2026]. See the Terms and Conditions (https://onlinelibrary.wiley.com/terms-and-conditions) on Wiley Online Library for rules of use; OA articles are governed by the applicable Creative Commons License

The authors report an LOD of 75 nM in spiked PBS and negligible interference of uric acid and various ions. The sensor was also tested in spiked urine samples that had undergone enzymatic treatment to convert 1OHP-gluc to free 1OHP, which is electroactive, detecting between 91.8% and 108% of the added concentration. A signal drop of over 20% was reported after storing the sensor for two weeks, showing that shelf stability is still a point of attention. A different framework based on zeolitic imidazolate (ZIF-8)/ionic liquid composites immobilized on carbon paste was also reported, detecting 1OHP electrooxidation using DPV [68]. ZIF-8 is a commercially available MOF based on zinc and methylimidazole linkers. The sensor achieved good shelf stability, an LOD of 10 nM in spiked phosphate-buffered saline (PBS) with pH = 9, and exhibited limited interference by uric acid, but no testing for cross-selectivity with other hydroxylated PAH metabolites (e.g., naphthol (OHN)) was reported [68]. Building on this, the authors reported a sensor based on a different commercial MOF, ZIF-67, which they decorated with colloidal Au and deposited onto a carbon nanofiber paste for detecting 1OHP using square-wave voltammetry (SWV) [69]. They reported an LOD of 0.1 nM in spiked water samples under optimized conditions, shelf stability, and reproducibility with the sensor detecting 99.6%–105.3% of 1OHP added to urine samples [69]. Despite this, the extensive sample pretreatment of buffering, enzymatic proteolysis including incubation, centrifugation, solvent extraction, and redissolution limit the applicability outside of a laboratory environment so far. An overview of the reviewed MOF-based sensors is listed in Table 3.

3.3 | Carbon Materials and Nanomaterials-Based Sensors

Carbon-based materials like glassy carbon and carbon nanostructures have been employed for successfully detecting PAHs and PAH metabolites for many years [83–85]. Using surface functionalization for, e.g., preconcentrating analytes, nanomolar detection of 1OHP was already achieved in 2011 [84], even avoiding interference by uric acid, but further lowering the LOD and ensuring high selectivity remains challenging. Carbon nanotubes (CNTs) were used to address this issue and increase the surface area for better sensitivity [86, 87], and graphene is even more interesting for electrochemical applications. Due to its outstanding properties, single-layer graphene has been employed in a variety of applications including electrocatalysis, energy conversion, and sensing since the elucidation of its properties in 2004 by Geim and Novoselov [88]. Besides the excellent electrocatalytic activity of pure and doped graphene as well as that of its derivatives such

TABLE 3 | Overview of MOF-based PAH sensors for 1OHP including the individual LODs, if reported.

Framework	LOD, nM	Notes	References
Eu^{3+} with Ga(OH)(benzenetetracarboxylic acid)-based linker	3.2	FQ; checked for interference; operable on paper support	[61]
Eu^{3+} with 4',4"'-oxybis([1,1'-biphenyl]-3,5-dicarboxylic acid-based linker	1100	FQ; LOD in real urine; also responds to tryptophane	[66]
Eu^{3+} with 2,6-di(2',5'-dicarboxylphenyl)pyridine-based linker	Unknown	FQ; in human urine; checked for interference by uric acid	[73]
Eu^{3+} with 5,5'-carbonyldiisophthalic acid-based linker	710	FQ; did not distinguish between response of uric acid and 1OHP, in human urine	[74]
Eu^{3+} with 5'-methyl-[1,1':3',1"-triphenyl]-3,3",5,5"-tetracarboxylic acid-based linker	1810	FQ; did not distinguish between response of uric acid and 1OHP, in human urine	[75]
Eu^{3+} with pentadecene octacarboxylate-based ligand	Unknown	FQ; measured 230 μM—did not report a LOD; no interference by uric acid	[76]
Eu^{3+} with multiple, consecutively introduced ligands	19	FQ; did not distinguish between response of Cu^{2+} and 1OHP; in water	[80]
Eu^{3+} with 5-triazole isophthalic acid-based ligands	150	FQ; LOD in urine, checked for interferants incl. uric acid	[81]
Tb^{3+} with 5-triazole isophthalic acid-based ligands	600	FQ; LOD in urine, checked for interferants incl. uric acid	[81]
Cd^{2+} with 5'-methyl-[1,1':3',1"-triphenyl]-3,3",5,5"-tetracarboxylic acid-based linker	710	FQ; LOD in urine, also detects tryptophane but cannot differentiate between them	[67]
Zn^{2+} with 4',4"'-oxybis([1,1'-biphenyl]-3,5-dicarboxylic acid-based linker	Unknown	FQ; in human urine, LOD given as quenching constant $K_{SV} = 5.79 \times 10^{-6}$ M^{-1}	[77]
Cr^{3+} with polyamidoamine-based linker on GO	75	DPV, checked for interference; extensive sample pretreatment	[70]
Zeolitic imidazole (ZIF-8) with ionic liquid on C paste	10	DPV, LOD in water, checked for interference and in 5 μM spiked urine	[68]
Zeolitic imidazole (ZIF-67) on C nanofibers	0.1	SWV, LOD in water, checked for interference and in 5 μM spiked urine samples	[69]

18626319, 2026, 17, Downloaded from https://onlinelibrary.wiley.com/doi/10.1002/pssa.70497 by Martin Konrad - Ku Leuven , Wiley Online Library on [07/09/2026]. See the Terms and Conditions (https://onlinelibrary.wiley.com/terms-and-conditions) on Wiley Online Library for rules of use; OA articles are governed by the applicable Creative Commons License

as GO or reduced graphene oxide (rGO) [89], it received attention for sensing PAHs and PAH metabolites due to its planar honeycomb lattice structure and completely delocalized π-electron system [90]. As PAHs and their hydroxylated derivates are planar with a mostly delocalized π-electron cloud, there is a direct interaction between them and graphene, which enables electrochemical sensing. The interaction is mostly based on an overlap between the π-electron cloud of graphene/GO and the π-electron cloud of PAHs and PAH metabolites [91], resulting in $\pi-\pi$ stacking, which forms the dominant interaction [92]. The interaction is depicted in Figure 8.

Graphene and related carbon materials, e.g., GO, can also facilitate binding via hydrogen bonds complementary to $\pi-\pi$ stacking, particularly between the hydroxy group of PAH metabolites like 1OHP or 1OHN and delocalized π-electron systems [70, 93, 94], both natively and following functionalization [95]. Surface functionalization also enables covalent and noncovalent binding as well as electrostatic interaction, all of which can occur in conjunction with $\pi-\pi$-stacking or hydrogen bonds [96]. Doping graphene, as well as deposition of nanoparticles on graphene, GO, or rGO can also facilitate improved charge transfer for better catalytic activity [96, 97].

As different PAHs and metabolites have different electrooxidation potentials ($U_{oxidation}$, e.g., 0.3 V_{SHE} for 1OHP compared to 0.7 V_{SHE} for 2OHN in PBS at pH = 4 [90]), some degree of selectivity can be achieved by determining the electrooxidation potential of individual compounds. This potential can be detected using electrochemical methods including cyclic voltammetry (CV), DPV, or SWV. These methods are sometimes used in conjunction with a ferrocyanide redox probe ($[Fe(CN)_6]^{3-/4-}$), where a shift in the potential of the ferrocyanide redox reaction is detected [84, 98, 99]. However, the precise electrooxidation potential also depends on matrix parameters such as pH, presence of ions, and other compounds, which limits the selectivity between structurally very similar compounds in untreated solutions or requires control of, e.g. the pH levels. In addition, some PAHs and PAH metabolites exhibit multiple oxidation peaks across a range of potentials corresponding to different oxidation steps of the molecules [82, 83].

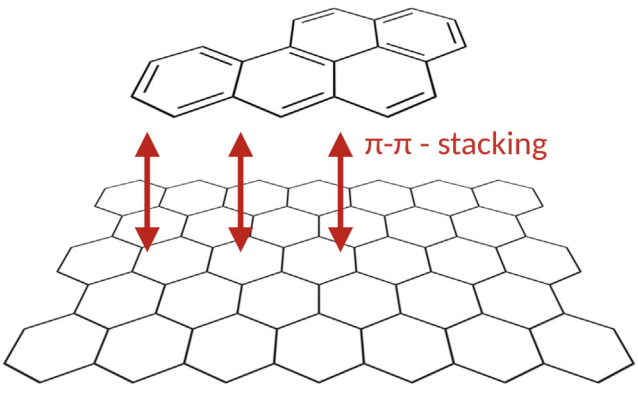

FIGURE 8 | Schematic depiction of interaction between graphene and benzo[*a*]pyrene based on $\pi-\pi$ stacking, which is possible due to the complete delocalization of π-electrons over the planar structure of graphene and the partial delocalization of π-electrons of B[*a*]P and other PAHs and PAH metabolites. Image created with biorender.com.

An early approach to sense urinary 1OHP electrochemically on carbon-based materials was by directly measuring its electrooxidation peaks on multiwalled carbon nanotubes (MWCNT) on a glassy carbon electrode via SWV [83]. The used urine sample was pretreated by alkaline hydrolysis, heating, and setting an acidic pH prior to extraction with hexane since various urine components were reported to interfere with this direct sensing approach without a recognition element. A LOD of 0.1 nM was reported, but the detection was fully dependent on the successful separation of 1OHP from other electroactive compounds like 1OHN prior to measurement.

One way to improve sensing performance is the incorporation of graphene into various materials for improved electrocatalytic performance. A Cu–GO hybrid material on a glassy carbon substrate was reported for direct electrochemical sensing of 2OHN using DPV with an LOD of 5 nM, with little interference from other organic molecules [89]. A similar direct oxidation approach based on graphene composites was reported using a carbon electrode modified with graphene in a hyper-crosslinked resin for a larger surface area and preconcentration of 1OHP at the sensor [100]. Achieving an LOD of 1.72 nM using DPV, neither various ions nor uric acid were found to interfere with the sensing performance, and the sensor could be successfully used to recover between 97.4% and 100.4% of added 1OHP from real urine samples collected from both smokers and nonsmokers, indicating very little interference by other PAH metabolites and other compounds expected in smokers' urine. Pang et al. reported the deposition of graphene by electrochemical reduction of GO onto a glassy carbon electrode,and subsequent preconcentration of 1OHP for direct electrochemical sensing using DPV, achieving a LOD of 0.84 nM in water and validating it in spiked and enzyme-treated urine against HPLC [101].

One obstacle in using graphene and monolayers of its derivatives like GO or rGO is the tendency of the individual layers to reaggregate into a 3D structure, reducing the available surface area and thus reducing its electrocatalytic activity [98]. One way to avoid this is by introducing intermediate layers as dopants that retain the π-conjugation. In one publication, octa(3-aminopropyl)octasilsesquioxane octahydrochloride has been used in conjunction with rGO nanoribbons to achieve an LOD for 1OHP of 40 nM [98]. This alternating-layer approach was also employed using poly-8-methoxy-7-methyl-5-(10-anthracen-9-yl) quinolone (PMMAYQ) and rGO for sensing 1OHP from pretreated urine [102]. By manufacturing an increased specific surface area using the dispersed rGO without losing its π-conjugated structure, the authors report an LOD of 0.07 nM for 1OHP. This approach was also used to develop a multisensor for 1OHP, 2OHN, and 3-OH phenanthrene (3OHPhen) based on graphene and a polyelectrolyte $PbCSO_3Na$ [85]. The authors report LODs of 1.43 nM (2OHN), 3.21 nM (3OHPhen), and 10.42 nM (1OHP), respectively, in pretreated samples. Focusing on ease of preparation and cost-effectiveness, the same group also developed a multisensor based on rGO on a screen-printed carbon electrode and detecting the same three compounds using their individual oxidation potentials, achieving LODs of 10.1 nM (2OHN), 15.3 nM (3OHPhen), and 20.4 nM (1OHP), respectively, in pretreated samples [90].

Differentiating between individual PAHs and metabolites can also be improved by introducing a recognition element such

18626319, 2026, 17, Downloaded from https://onlinelibrary.wiley.com/doi/10.1002/pssa.70497 by Martin Konrad - Ku Leuven , Wiley Online Library on [07/09/2026]. See the Terms and Conditions (https://onlinelibrary.wiley.com/terms-and-conditions) on Wiley Online Library for rules of use; OA articles are governed by the applicable Creative Commons License

as cyclodextrins (CDs) [103]. CDs are cyclic oligosaccharides composed of glucose units in a conical shape with a hydrophobic interior and hydrophilic exterior [104]. This structure enables a host–guest interaction between them and hydrophobic molecules that enter the CD's cone based on size exclusion. This approach was used for the development of electrochemical sensors [105]. CDs were also used to capture PAHs from liquid media via adsorption [106]. Based on this, a sensor using Au nanoparticles/hollow nitrogen-doped carbon microsphere hybrids functionalized with thiolated-β-CDs as recognition elements for selective sensing of 1- and 2-naphththol was developed [103]. Differentiating the two naphthols by the potentials of their respective oxidation peaks, a LOD of 1 nM (1OHN) and 1.2 nM (2OHN) in spiked aquatic samples is reported, with good recovery and satisfactory congruence with results from HPLC. Another sensor for selectively detecting 1- and 2OHN by their individual oxidation potentials was reported based on 3D graphene nanostructures [107]. Achieving a LOD of 10 nM (1OHN) and 20 nM (2OHN), the sensor also exhibited no interference from multiple compounds including uric acid in spiked urine samples. A similar sensor based on rGO was also reported, achieving an LOD of 1.01 nM (1OHN) and 0.43 nM (2OHN) [99].

Using a screen-printed graphene electrode as substrate and modifying it with electropolymerized poly(*L*-glutamic acid), a sensor capable of detecting 1OHP from human urine using a $[Fe(CN)_6]^{3-/4-}$ redox probe with a LOD of 0.95 nM was reported [108]. The sensor exhibited no interference from uric acid, creatinine, or other common components of urine, but the authors of ref. [108] did not report on the effect of possible competitors like naphthol. Graphene has also been used to construct a field-effect transistor for detecting pyrene [109]. Again, the binding of the analyte is based on $\pi-\pi$ interactions, but a binding event is detected as a shift in the Dirac point (the potential at which the conduction band and the valence band meet) due to the analyte acting as a *N*-type dopant. While a low LOD of 0.1 nM and a very good stability are reported, the sensor is not reported to differentiate between different PAHs [109]. Another option is the use of graphene quantum dots (GQDs) and their fluorescence for sensing pyrene [110]. Demonstrating a proof-of-concept, GQDs were prepared using both bottom-up (pyrolysis and carbonization of citric acid) and top-down (oxidation of GO) approaches. The innate fluorescence of GQDs is based on radiative recombination of electron–hole pairs in sp^2-hybridized carbon atoms of the GQDs [110]. This fluorescence is quenched by adding iron (Fe^{3+}) ions—an effect the authors attribute to coordination with OH groups at the GQD surface, leading to aggregation with neighboring GQDs. The presence of pyrene disrupts these aggregates as the interaction between the analyte and GQDs based on $\pi-\pi$ stacking is energetically favored, thus enhancing fluorescence. The authors report an LOD of

TABLE 4 | Overview of carbon-based sensors for PAHs and PAH metabolites, using glassy carbon materials, graphene, graphene oxide (GO) or reduced graphene oxide (rGO). $U_{oxidation}$ describes the electrooxidation potential of a given analyte.

Recognition element	Target	LOD, nM	Notes	References
MWCNT on glassy carbon	1OHP	0.1	SWV, in extraction from pretreated urine	[83]
Glassy carbon modified with poly(3-methylthiophene)	1OHP	165	DPV with $[Fe(CN)_6]^{3-/4-}$	[84]
β-Cyclodextrin on glassy carbon microspheres	1OHN, 2OHN	1.0	DPV, in spiked water, differentiated by $U_{oxidation}$	[103]
Graphene with resin	1OHP	1.72	CV and DPV	[100]
L-Glutamic acid on graphene	1OHP	3.16	Checked for interferants incl. uric acid	[108]
$PbCSO_3Na$/graphene multilayer	Multiple hydroxylated PAHs	1.43	DPV with $[Fe(CN)_6]^{3-/4-}$, differentiated by $U_{oxidation}$	[85]
Graphene	Pyrene	0.1	Field effect transistor, utilizes changes in Dirac point	[109]
Graphene in 3D nanostructure	1OHN and 2OHN	10	DPV with $[Fe(CN)_6]^{3-/4-}$	[107]
Graphene quantum dots	Pyrene	242	Fluorescence-based	[110]
Cu nanostructures on GO	2OHN	5	DPV, tested in real urine	[89]
GO nanoribbons	1OHP	40	DPV with $[Fe(CN)_6]^{3-/4-}$	[98]
rGO	1OHN, 2OHN	0.4	DPV + $[Fe(CN)_6]^{3-/4-}$, differentiated by $U_{oxidation}$	[99]
rGO	1OHP	0.84	DPV with $[Fe(CN)_6]^{3-/4-}$	[101]
rGO + conjugated PMMAYQ multilayer	1OHP	0.07	DPV with $[Fe(CN)_6]^{3-/4-}$	[102]
rGO on carbon electrode	Multiple hydroxylated PAHs	0.84	DPV with $[Fe(CN)_6]^{3-/4-}$, differentiated by $U_{oxidation}$	[90]
rGO + calixarene on carbon electrode	Anthracene	0.016	DPV, LOD approximated by extending calibration curve	[102]

18626319, 2026, 17, Downloaded from https://onlinelibrary.wiley.com/doi/10.1002/pssa.70497 by Martin Konrad - Ku Leuven , Wiley Online Library on [07/09/2026]. See the Terms and Conditions (https://onlinelibrary.wiley.com/terms-and-conditions) on Wiley Online Library for rules of use; OA articles are governed by the applicable Creative Commons License

351 nM for the top-down fabricated sensor and of 242 nM for the bottom-up fabricated one, without testing for possible interference by other PAHs. An overview of the reviewed carbon nanomaterial-based sensors is listed in Table 4.

3.4 | PAHs and Similar Compounds as Recognition Elements

Building on the interactions between graphene and other planar systems with PAHs, Muñoz et al. developed an impedimetric sensor based on immobilizing the target molecule itself on a self-assembling monolayer (SAM) on ITO as a homologous recognition element for selective sensing in presence of a redox marker [111]. Binding of the target occurs due to the planar and aromatic nature of PAHs, which enable a stacking of the molecules on top of one another due to π-interactions between the aromatic systems [111]—similar as in graphene-based sensors—but with increased selectivity. Using pyrene as model molecule, a LOD of 9 pM in water was reported, with limited interference by other PAHs [111]. The authors attribute the exceptionally low LOD to the combination of using a monolayer of the recognition element in conjunction with electrochemical impedance spectroscopy (EIS) as sensing technique, which is very sensitive in detecting changes of electrode properties [112]—in this case, a change in charge transfer resistance upon binding of the analyte. A follow-up study using CNTs instead of PAHs as recognition elements corresponds to this, achieving a pM LOD for PAHs as well but being nonspecific to individual PAHs [87]. Building on this, the authors developed a multisensor based on four individually SAM-functionalized sensing sites for naphthalene, anthracene, pyrene, and fluoranthene in one integrated sensor, utilizing epoxy groups on silane for anchoring the detection unit [113]. The individual SAMs on each individual sensing site contained one of the four target analytes to utilize the preferential binding of PAHs with identical molecules over other PAHs. The sensor exhibited no cross-selectivity or false positives for additional PAHs in water, achieving LODs in the picomolar range. The method shows promise for developing a portable, accurate, and selective sensor to measure PAHs in aquatic samples. An overview of the reviewed sensors based on PAHs as recognition elements is listed in Table 5.

3.5 | Molecularly Imprinted Polymers (MIPs)

MIPs are synthetic bioreceptors that detect their target analytes via a lock-and-key mechanism [114]. The monomers forming the MIP are polymerized in presence of a so-called "imprinting template"—most commonly the target analyte. As they polymerize, the polymer is formed around the imprinting template and solidifies. Subsequent extraction (e.g., using a suitable solvent that can remove the imprinting template from the polymer matrix without damaging it) of the imprinting template reveals complementary nanocavities in the polymer: the binding sites [115]. If the target analyte is present in a sample, geometrical and steric constraints lead to selective binding in the cavity via hydrogen bonds, π–π interactions, dipole interactions, and/or van der Waals forces [116, 117]. The analyte binding will then trigger a change in electrical, physical, or chemical parameters, which enables sensing. The principle behind MIP synthesis and sensing is depicted in Figure 9.

Besides their selectivity and aptitude for customization, MIPs exhibit high chemical and physical stability, making them well suited for application in complex media [118–120]. For detecting PAHs and their metabolite, π–π interactions and geometrical constraints of the cavities are by far the most important contributors to selective and sensitive detection as most recently developed MIPs are based on polymers with delocalized π-electrons, like in polypyrrole (PPy) or polyaniline. Besides application as a recognition element, MIPs were also investigated as solid phase for extracting PAHs in laboratory setups due to their high selectivity and affinity for their target molecules [121].

MIPs were utilized for luminescence-based sensing, albeit usually in a laboratory-based context due to the required optical

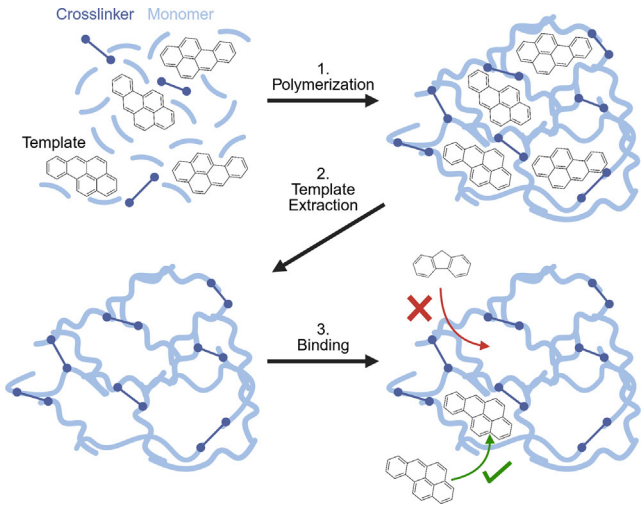

FIGURE 9 | Schematic depiction of MIP synthesis and selective binding. A polymer is formed around the imprinting template, which is usually the target molecule the sensor is designed for. After extraction of the imprinting template is removed, cavities with suitable shape, size, and functionalizations remain that enable specific binding with the target analyte. Image created with biorender.com.

TABLE 5 | Overview of contemporary sensors using PAHs or similar molecules as recognition elements.

Substrate	Target	LOD, nM	Notes	References
Pyrene as self-assembled monolayer on ITO	Pyrene	0.009	EIS with $[Fe(CN)_6]^{3-/4-}$ probe	[111]
CNTs on SAM on ITO	Multiple PAHs	0.009	EIS with $[Fe(CN)_6]^{3-/4-}$ probe	[87]
PAHs on SAM on ITO	Multiple PAHs	0.006	EIS with $[Fe(CN)_6]^{3-/4-}$ probe, array sensing	[113]

18626319, 2026, 17, Downloaded from https://onlinelibrary.wiley.com/doi/10.1002/pssa.70497 by Martin Konrad - Ku Leuven , Wiley Online Library on [07/09/2026]. See the Terms and Conditions (https://onlinelibrary.wiley.com/terms-and-conditions) on Wiley Online Library for rules of use; OA articles are governed by the applicable Creative Commons License

TABLE 6 | Overview of contemporary MIP-based sensors for PAH/PAH-metabolites.

Polymer	Target	LOD, nM	Notes	References
TiO_2 sol–gel	1OHP	0.35	Imprinted sol–gel	[132]
o-Phenylenediamine	1OHN	1.5	DPV using a $[Fe(CN)_6]^{3-/4-}$ probe; checked for interference	[128]
Bisphenol A—methylene diphenyl diisocyanate	B[*a*]P	0.2	Luminescence quenching-based	[122]
Bisphenol A—methylene diphenyl diisocyanate	Anthracene	1.3	Conductometric	[125]
Ferrocenylmethyl methacrylate	B[*a*]P	0.19	DPV without redox probe used for sensing	[129]
Polystyrene-co-methacrylic acid + $LaVO_3$:Eu	Phenanthrene	20	Luminescence quenching & magnetic separation	[123]
PPy	Anthracene	12	SWV used for sensing	[127]
PPy	Pyrene	200	Direct CV used for sensing	[126]
Polythiophene	Pyrene	Not reported	Fluorescence-based, linear response until 10 nM	[124]

setups and/or extensive sample processing. Using a MIP based on bisphenol A and methylene diphenyl diisocyanate, a sensor for B[*a*]P based on the emission intensity after excitation with UV light was reported [122]. The sensor achieved a LOD of 0.2 nM, and limited interference from other PAHs is reported when measuring the phosphorescence response, but significant interference is detected upon measuring the fluorescence response [122].

In a different approach, an amphiphilic copolymer matrix based on polystyrene-co-methacrylic acid incorporating Fe_3O_4 nanoparticles for hydrophobicity and La:VO_4:Eu nanoparticles for fluorescence was reported [123]. Phenanthrene was used as imprinting template, and addition of a solution of PAHs such as pyrene as well as the target phenanthrene induced a quenching in fluorescence intensity. Magnetic separation of the magnetic nanocomposites and the sample matrix revealed that phenanthrene continues to quench fluorescence, whereas competing PAHs stop quenching, which enables the selective detection of phenanthrene. Achieving an LOD of 20 nM, the sensor was also successfully tested in milk samples. A fluorescence-based sensor using a polythiophene-based MIP nanofilm was also reported [124]. There, the emitted fluorescence is proportional to the concentration of pyrene in an aquatic samples, and pyrene could be differentiated from its competitors B[*a*]P and chrysene based on the emission wavelength. A LOD was not reported, but a linear response was stated down to a concentration of 10 nM. MIPs were also utilized for the electrochemical detection of 1OHP, which is more promising than optical methods for miniaturization and field use. A conductometric sensor utilizing a polyurethane-based MIP as recognition element for anthracene in NaCl as supporting electrolyte has been reported, achieving a LOD of 1.3 nM [125]. More commonly, the measured current intensity at the electrooxidation potential of the target analyte measured using CV, SWV, or DPV is used for electrochemically detecting PAHs and their metabolites with MIPs. A PPy-based MIP using CV for detecting pyrene in aquatic samples with an LOD of 0.2 µM was reported [126]. Also using PPy as polymer, Mathieu-Scheers et al. developed a sensor for detecting anthracene in aquatic media via SWV with a LOD of 12 nM [127]. The sensor was affected by interference from similar PAHs like B[*a*]P only when their concentration was twice as large as the target analytes' concentration. Similarly, Bartilotti et al. reported an *o*-phenylenediamine-based MIP for detecting 1OHN in water samples using DPV in combination with a $[Fe(CN)_6]^{3-/4-}$ probe, achieving a LOD of 1.5 nM and limited interference by competing species such as the analyte's parent PAH, naphthalene [128]. Ibrahim et al. developed a polymer based on ferrocenylmethyl methacrylate, which acted as functional monomer as well as redox probe for detecting the target B[*a*]P using DPV [129]. Photoiniferter polymerization was used, which is based on initiating, controlling, and terminating radical polymerization via a thiocarbonylthio compound that forms radicals upon light exposure and can be used for anchoring SAMs to surfaces [130, 131]. Grafting the polymer onto a Au electrode by forming a SAM and subsequently initiating the polymerization, they achieved a LOD of 0.19 nM in potassium chloride solution. Imprinting into a sol–gel instead of a typical polymer, an electrochemical 1OHP sensor based on an a MIP—titanium dioxide (TiO_2) gel matrix has been reported as well, following the same principle as MIPs [132]. Sensing was done using CV in combination with a $[Fe(CN)_6]^{3-/4-}$ probe, achieving a LOD of 0.3 nM, albeit some interference by similar molecules like pyrene was reported. An overview of the reviewed sensors based on molecular imprinting is listed in Table 6.

4 | Conclusion and Outlook

Concerns about individual health and environmental pollution have led to a considerable amount of research on PAH and PAH metabolite sensing in recent years. Despite exhibiting shortcomings regarding ease of use, cost, and measurement duration, laboratory-based methodologies remain the gold standard for clinical studies and incidental analysis—and with recent advances regarding throughput, analysis time, and novel detectors, they will probably remain the point of reference for the time being. SERS-based detectors also gathered a lot of attention in recent years but still rely on efficient analyte separation prior

18626319, 2026, 17, Downloaded from https://onlinelibrary.wiley.com/doi/10.1002/pssa.70497 by Martin Konrad - Ku Leuven , Wiley Online Library on [07/09/2026]. See the Terms and Conditions (https://onlinelibrary.wiley.com/terms-and-conditions) on Wiley Online Library for rules of use; OA articles are governed by the applicable Creative Commons License

to analysis. Trapping the target analyte has so far been mostly based on hydrophobic bonds and $\pi-\pi$ stacking, making SERS mostly suitable for nonhydroxylated PAHs. Portable sensing made great progress, utilizing a plethora of different sensing mechanisms, each with its individual advantages and downsides. Biological recognition elements like antibodies or aptamers offer a very high selectivity at the expense of stability in different media and can be used both for PAHs and their metabolites, depending on the recognition element. MOF-based sensors are suitable for detecting the PAH metabolite 1OHP and exhibit great versatility in construction and sensing methods. However, they are often insufficiently sensitive for concentrations encountered in urinary or environmental samples or suffer from the interference of uric acid with fluorescence-based detection in particular. MIP-based sensors exhibit great robustness in complex media and very low LODs, but adapting them for field use remains a challenge. They can be ad hoc developed for both PAHs and hydroxylated metabolites, but the polymer choice is essential for ensuring effective binding (utilizing, e.g., noncovalent interaction or hydrogen bonding in conjunction with $\pi-\pi$ stacking) of the target analyte while maintaining the required conductivity or luminescence. Carbon-based materials and nanomaterials-based sensors utilizing electrochemical detection show great promise for field use and exhibit very low LOD for PAHs already, but the nonspecific interaction of the π-electron clouds remains a challenge for discriminating between structurally similar analytes. They are suited for both detection of PAHs and hydroxylated metabolites, with the latter significantly benefitting from functionalization or doping to enable the formation of hydrogen bonds and noncovalent bonds. Detecting the electrooxidation of different PAHs at their different potentials can help to alleviate this issue, but the oxidation potential is strongly pH-dependent. The integration of a multisensor including pH measurement could help further improve the real-life usability. Furthermore, the ubiquity of smartphones coupled with machine learning and artificial intelligence utilization for data analysis promises to enable sensors that are more sensitive, accurate, fast, and easier to operate to detect PAHs, their metabolites, or other substances of interest in various complex media.

Future sensors can fill different application nichés—from quick qualitative assessment to detailed paneling of multiple PAHs from a single sample. Balancing sensitivity and selectivity on one hand with ease of transport and use will determine their aptitude for complementing laboratory-based detection to enable easy, fast, and most importantly reliable detection of PAHs and their metabolites. In addition, the reviewed portable sensing technologies can be utilized for point-of-need sensing of other environmental pollutants as well. Sensors for endocrine disruptors such as bisphenol A [133, 134], estradiol [135, 136], glyphosate [137, 138], and dichlorodiphenyltrichloroethane, a commonly used pesticide [139, 140], have been reported. Other relevant substances of concern that could be detected are "forever chemicals" like polyfluoroalkyl substances [141, 142] or biogene amines [143].

Beyond that, many different compounds can be detected in urine samples using the techniques reviewed herein for sensing urinary PAH metabolites since the challenges of operating in this complex medium are similar for other analytes: SERS can be employed for detecting multiple urinary biomarkers linked to ischemic stroke [144]. Aptamers showed aptitude for detecting pesticide exposure from testing urine samples [145]. MOFs have been reported for luminescence-based sensing of tumor biomarkers [146] as well as for electrochemical sensing of creatinine as a marker of kidney failure [147]. Various carbon-based materials can be used for uric acid sensing [148]. MIPs can be used to detect analytes, including glucose [149] and illicit drugs [150].

These are just a few examples, illustrating the adaptability and transferability of these techniques and the findings resulting from developing sensors for complex media since every electrochemical sensor that is operating in urine has to account for the complexity of the medium, such as varying pH, matrix effects, and selectivity, which makes proper calibration and sufficient reproducibility challenging. Beyond the development stage of the sensor itself, the production process has to be optimized as well to minimize manufacturing variability. Reliable production and strict quality control are essential to deliver a reliable sensor to users and comply with legal requirements, especially for sensors used in the medical field.

Author Contributions

Martin Wolfgang Konrad: conceptualization, funding acquisition, investigation, visualization, writing – original draft preparation, writing – review and editing. **Jeroen Vanoirbeek:** conceptualization, funding acquisition, investigation, writing – original draft preparation, writing – review and editing. **Patrick Wagner:** conceptualization, funding acquisition, investigation, writing – original draft preparation, writing – review and editing. **Irene Taurino:** conceptualization, funding acquisition, investigation, writing – original draft preparation, writing – review and editing.

Acknowledgments

The authors gratefully acknowledge funding from the Research Foundation Flanders (FWO) (Ph.D. fellowship 1S81626N) and the Industrial Research Funds (IOF) of KU Leuven (Grant C3/23/022).

Funding

This work was supported by the Research Foundation Flanders (FWO) (1S81626N) and KU Leuven (C3/23/022).

Conflicts of Interest

The authors declare no conflicts of interest.

Data Availability Statement

Data sharing is not applicable to this article as no datasets were generated or analyzed during the current study.

References

1. "Regulation (EC) No 1907/2006 of the European Parliament and of the Council of 18 December 2006 Concerning the Registration, Evaluation, Authorisation and Restriction of Chemicals (REACH) - Updated Version From 2025," accessed March 3, 2026, https://eur-lex.europa.eu/legal-content/EN/TXT/?uri=CELEX:.

18626319, 2026, 17, Downloaded from https://onlinelibrary.wiley.com/doi/10.1002/pssa.70497 by Martin Konrad - Ku Leuven , Wiley Online Library on [07/09/2026]. See the Terms and Conditions (https://onlinelibrary.wiley.com/terms-and-conditions) on Wiley Online Library for rules of use; OA articles are governed by the applicable Creative Commons License

2. “US Agency for Toxic Substances and Disease Registry: Polycyclic Aromatic Hydrocarbons (PAHs),” accessed March 10, 2026, https://wwwn.cdc.gov/tsp/substances/ToxSubstance.aspx?toxid=25.

3. “Air Pollution Control Act (Act. No 97 of 1968) - Updated Version from 2017,” accessed May 18, 2026, https://www.japaneselawtranslation.go.jp/en/laws/view/4601.

4. G. Karavalakis, G. Fontaras, D. Ampatzoglou, et al., “Effects of Low Concentration Biodiesel Blends Application on Modern Passenger Cars. Part 3: Impact on PAH, Nitro-PAH, and Oxy-PAH Emissions,” *Environmental Pollution* 158 (2010): 1584–1594, https://doi.org/10.1016/j.envpol.2009.12.017.

5. K. Ravindra, R. Sokhi, and R. Van Grieken, “Atmospheric Polycyclic Aromatic Hydrocarbons: Source Attribution, Emission Factors and Regulation,” *Atmospheric Environment* 42 (2008): 2895–2921, https://doi.org/10.1016/j.atmosenv.2007.12.010.

6. K. Szramowiat-Sala, M. Marczak-Grzesik, M. Karczewski, M. Kistler, A. Kasper-Giebl, and K. Styszko, “Chemical Investigation of Polycyclic Aromatic Hydrocarbon Sources in an Urban Area With Complex Air Quality Challenges,” *Scientific Reports* 15 (2025): 6987, https://doi.org/10.1038/s41598-025-91018-8.

7. W. Li, D. Chen, Y. Peng, Z. Lu, and D. Wang, “Association of Polycyclic Aromatic Hydrocarbons With Systemic Inflammation and Metabolic Syndrome and Its Components,” *Obesity* 31, no. 5 (2023): 1392–1401, https://doi.org/10.1002/oby.v31.5.

8. C. Hoppe-Jones, S. C. Griffin, J. J. Gulotta, et al., “Evaluation of Fireground Exposures Using Urinary PAH Metabolites,” *Journal of Exposure Science & Environmental Epidemiology* 31 (2021): 913–922, https://doi.org/10.1038/s41370-021-00311-x.

9. Y. Chen, Y. Li, W. Gu, et al., “The Key Metabolic Signatures and Biomarkers of Polycyclic Aromatic Hydrocarbon-Induced Blood Glucose Elevation in Chinese Individuals Exposed to Diesel Engine Exhaust,” *Ecotoxicology and Environmental Safety* 284 (2024): 116997, https://doi.org/10.1016/j.ecoenv.2024.116997.

10. M. H. G. Andersen, A. T. Saber, J. E. Pedersen, et al., “Assessment of Polycyclic Aromatic Hydrocarbon Exposure, Lung Function, Systemic Inflammation, and Genotoxicity in Peripheral Blood Mononuclear Cells From Firefighters Before and After a Work Shift,” *Environmental and Molecular Mutagenesis* 59 (2018): 539–548, https://doi.org/10.1002/em.v59.6.

11. Y. Yang, Y. Li, Q. Xie, et al., “Evaluating the Kinetics and Molecular Mechanism for Biomimetic Metabolic Activation of PAHs by Surface-Enhanced Raman Scattering Spectroscopy,” *Analytical Chemistry* 96 (2024): 10365–10372, https://doi.org/10.1021/acs.analchem.4c01437.

12. K.-H. Kim, S. A. Jahan, E. Kabir, and R. J. C. Brown, “A Review of Airborne Polycyclic Aromatic Hydrocarbons (PAHs) and Their Human Health Effects,” *Environment International* 60 (2013): 71–80, https://doi.org/10.1016/j.envint.2013.07.019.

13. International Agency for Research on Cancer (IARC), “Occupational Exposure as a Firefighter,” *IARC Monographs on the Identification of Carcinogenic Hazards to Humans* 132 (2023): 1.

14. P. Zangl, C. Collart, and R. Persoons, “Air, Skin, and Biological Monitoring of French Fire Instructors’ Exposure to Particles/PAHs During Controlled Fire and Mitigation Strategies,” *Toxics* 13 (2025): 106, https://doi.org/10.3390/toxics13020106.

15. E. Pukkala, J. I. Martinsen, E. Weiderpass, et al., “Cancer Incidence Among Firefighters: 45 Years of Follow-up in Five Nordic Countries,” *Occupational and Environmental Medicine* 71 (2014): 398–404, https://doi.org/10.1136/oemed-2013-101803.

16. P. N. S. Zainal, S. A. A. Ahmad, S. F. N. A. Aziz, and N. Z. Rosly, “Polycyclic Aromatic Hydrocarbons: Occurrence, Electroanalysis, Challenges, and Future Outlooks,” *Critical Reviews in Analytical Chemistry* 52 (2022): 878–896, https://doi.org/10.1080/10408347.2020.1839736.

17. F. J. Jongeneelen, “Benchmark Guideline for Urinary 1-Hydroxypyrene as Biomarker of Occupational Exposure to Polycyclic Aromatic Hydrocarbons,” *The Annals of Occupational Hygiene* 45, no. 1 (2001): 3–13, https://doi.org/10.1016/S0003-4878(00)00009-0.

18. F. J. Jongeneelen, R. B. M. Anzion, and P. T. Henderson, “Determination of Hydroxylated Metabolites of Polycyclic Aromatic Hydrocarbons in Urine,” *Journal of Chromatography B: Biomedical Sciences and Applications* 413 (1987): 227–232, https://doi.org/10.1016/0378-4347(87)80230-X.

19. H. Louro, B. C. Gomes, A. T. Saber, et al., “The Use of Human Biomonitoring to Assess Occupational Exposure to PAHs in Europe: A Comprehensive Review,” *Toxics* 10 (2022): 480, https://doi.org/10.3390/toxics10080480.

20. S. McCormick, J. E. Snawder, I.-C. Chen, et al., “Exposure Assessment of Polycyclic Aromatic Hydrocarbons in Refined Coal Tar Sealant Applications,” *International Journal of Hygiene and Environmental Health* 242 (2022): 113971, https://doi.org/10.1016/j.ijheh.2022.113971.

21. S. F. Fernández, O. Pardo, C. S. Hernández, B. Garlito, and V. Yusà, “Children’s Exposure to Polycyclic Aromatic Hydrocarbons in the Valencian Region (Spain): Urinary Levels, Predictors of Exposure and Risk Assessment,” *Environment International* 153 (2021): 106535, https://doi.org/10.1016/j.envint.2021.106535.

22. “US Agency for Toxic Substances & Disease Registry (ATSDR),” accessed June 09, 2026, https://www.atsdr.cdc.gov/programs/substance-priority-list.html?CDC_AAref_Val=https://www.atsdr.cdc.gov/spl/.

23. L. H. Keith, “The Source of U.S. EPA’s Sixteen PAH Priority Pollutants,” *Polycyclic Aromatic Compounds* 35 (2015): 147–160, https://doi.org/10.1080/10406638.2014.892886.

24. J. T. Andersson and C. Achten, “Time to Say Goodbye to the 16 EPA PAHs? Toward an up-to-Date Use of PACs for Environmental Purposes,” *Polycyclic Aromatic Compounds* 35 (2015): 330–354, https://doi.org/10.1080/10406638.2014.991042.

25. B. A. Rybicki, N. L. Nock, A. T. Savera, D. Tang, and A. Rundle, “Polycyclic Aromatic Hydrocarbon-DNA Adduct Formation in Prostate Carcinogenesis,” *Cancer Letters* 239 (2006): 157, https://doi.org/10.1016/j.canlet.2005.07.029.

26. P. Sims, P. L. Grover, A. Swaisland, K. Pal, and A. Hewer, “Metabolic Activation of Benzo (a) Pyrene Proceeds by a Diol-Epoxide,” *Nature* 252 (1974): 326–328, https://doi.org/10.1038/252326a0.

27. J. L. Durant, A. L. Lafleur, W. F. Busby Jr, L. L. Donhoffner, B. W. Penman, and C. L. Crespi, “Mutagenicity of $C_{24}H_{14}$ PAH in Human Cells Expressing CYP1A1,” *Mutation Research/Genetic Toxicology and Environmental Mutagenesis* 446 (1999): 1–14, https://doi.org/10.1016/S1383-5718(99)00135-7.

28. D. Wang, A. Groot, A. Seidel, et al., “The Influence of Alkyl Substitution on the In Vitro Metabolism and Mutagenicity of Benzo[a] pyrene,” *Chemico-Biological Interactions* 363 (2022): 110007, https://doi.org/10.1016/j.cbi.2022.110007.

29. M. A. Mallah, L. Changxing, M. A. Mallah, et al., “Polycyclic Aromatic Hydrocarbon and Its Effects on Human Health: An Overview,” *Chemosphere* 296 (2022): 133948, https://doi.org/10.1016/j.chemosphere.2022.133948.

30. B. K. Behera, A. Das, D. J. Sarkar, et al., “Polycyclic Aromatic Hydrocarbons (PAHs) in Inland Aquatic Ecosystems: Perils and Remedies Through Biosensors and Bioremediation,” *Environmental Pollution* 241 (2018): 212–233, https://doi.org/10.1016/j.envpol.2018.05.016.

31. I. R. Comnea-Stancu, J. F. van Staden, and R.-I. S. van Staden, “Review - Trends in Recent Developments in Electrochemical Sensors for the Determination of Polycyclic Aromatic Hydrocarbons From Water Resources and Catchment Areas,” *Journal of the Electrochemical Society* 168 (2021): 047504, https://doi.org/10.1149/1945-7111/abf260.

18626319, 2026, 17, Downloaded from https://onlinelibrary.wiley.com/doi/10.1002/pssa.70497 by Martin Konrad - Ku Leuven , Wiley Online Library on [07/09/2026]. See the Terms and Conditions (https://onlinelibrary.wiley.com/terms-and-conditions) on Wiley Online Library for rules of use; OA articles are governed by the applicable Creative Commons License

32. S. A. Nsibande, H. Montaseri, and P. B. C. Forbes, "Advances in the Application of Nanomaterial-Based Sensors for Detection of Polycyclic Aromatic Hydrocarbons in Aquatic Systems," *TrAC Trends in Analytical Chemistry* 115 (2019): 52–69, https://doi.org/10.1016/j.trac.2019.03.029.

33. Å. M. Hansen, O. M. Poulsen, J. M. Christensen, and S. H. Hansen, "Determination of 1-Hydroxypyrene in Human Urine by High-Performance Liquid Chromatography," *Journal of Analytical Toxicology* 17 (1993): 38–41, https://doi.org/10.1093/jat/17.1.38.

34. G. Lux, A. Langer, M. Pschenitza, et al., "Detection of the Carcinogenic Water Pollutant Benzo [a] Pyrene With an Electro-Switchable Biosurface," *Analytical Chemistry* 87 (2015): 4538–4545, https://doi.org/10.1021/acs.analchem.5b00648.

35. S. Felemban, P. Vazquez, and E. Moore, "Future Trends for In Situ Monitoring of Polycyclic Aromatic Hydrocarbons in Water Sources: The Role of Immunosensing Techniques," *Biosensors* 9 (2019): 142, https://doi.org/10.3390/bios9040142.

36. M. Frederiksen, S. P. Jensen, M. H. G. Andersen, U. Vogel, and A. T. Saber, "Online SPE-LC-MS-MS Method for Eight Hydroxylated Metabolites of Polycyclic Aromatic Hydrocarbons in Urine and Determination of Optimal Sampling Time After Firefighter Training," *Toxicology Letters* 400 (2024): 9–15, https://doi.org/10.1016/j.toxlet.2024.07.005.

37. Q. Zhang, P. Liu, S. Li, X. Zhang, and M. Chen, "Progress in the Analytical Research Methods of Polycyclic Aromatic Hydrocarbons (PAHs)," *Journal of Liquid Chromatography & Related Technologies* 43 (2020): 425–444, https://doi.org/10.1080/10826076.2020.1746668.

38. Y. Zhang, L. Yuan, S. He, et al., "Contemporary Research Progress on the Detection of Polycyclic Aromatic Hydrocarbons," *International Journal of Environmental Research and Public Health* 19 (2022): 2790, https://doi.org/10.3390/ijerph19052790.

39. R. Fan, Y. Dong, W. Zhang, et al., "Fast Simultaneous Determination of Urinary 1-Hydroxypyrene and 3-Hydroxybenzo[a]pyrene by Liquid Chromatography-Tandem Mass Spectrometry," *Journal of Chromatography B* 836 (2006): 92–97, https://doi.org/10.1016/j.jchromb.2006.03.044.

40. Z. Li, L. C. Romanoff, D. A. Trinidad, et al., "Measurement of Urinary Monohydroxy Polycyclic Aromatic Hydrocarbons Using Automated Liquid-Liquid Extraction and Gas Chromatography / Isotope Dilution High-Resolution Mass Spectrometry," *Analytical Chemistry* 78 (2006): 5744, https://doi.org/10.1021/ac0606094.

41. A. P. W. Banks, P. Thai, M. Engelsman, X. Wang, A. F. Osorio, and J. F. Mueller, "Characterising the Exposure of Australian Firefighters to Polycyclic Aromatic Hydrocarbons Generated in Simulated Compartment Fires," *International Journal of Hygiene and Environmental Health* 231 (2021): 113637, https://doi.org/10.1016/j.ijheh.2020.113637.

42. H.-W. Chen, "Determination of 1-Hydroxypyrene in Human Urine by Acid Hydrolysis Coupled to Solid-Phase Microextraction and Semi-Microcolumn Liquid Chromatography," *Analytical Sciences* 23 (2007): 1221–1225, https://doi.org/10.2116/analsci.23.1221.

43. Y. Wang, L. Meng, E. N. Pittman, et al., "Quantification of Urinary Mono-Hydroxylated Metabolites of Polycyclic Aromatic Hydrocarbons by on-Line Solid Phase Extraction-High Performance Liquid Chromatography-Tandem Mass Spectrometry," *Analytical and Bioanalytical Chemistry* 409 (2017): 931–937, https://doi.org/10.1007/s00216-016-9933-x.

44. P. T. Strickland, D. Kang, E. D. Bowman, et al., "Identification of 1-Hydroxypyrene Glucuronide as a Major Pyrene Metabolite in Human Urine by Synchronous Fluorescence Spectroscopy and Gas Chromatography-Mass Spectrometry," *Carcinogenesis* 15 (1994): 483–487, https://doi.org/10.1093/carcin/15.3.483.

45. L. Chen, X. Tian, Y. Li, C. Yang, Y. Huang, and Y. Nie, "Rapid and Sensitive Screening of Multiple Polycyclic Aromatic Hydrocarbons by a Reusable Fluorescent Sensor Array," *Journal of Hazardous Materials* 424 (2022): 127694, https://doi.org/10.1016/j.jhazmat.2021.127694.

46. C. Wang, T. Sha, J. Lu, Y. Wang, Y. Guan, and X. Geng, "A Compact and Highly Sensitive Multi-Channel Deep UV LED-Induced Fluorescence Detector for PAHs Detection," *Sensors and Actuators B: Chemical* 442 (2025): 138180, https://doi.org/10.1016/j.snb.2025.138180.

47. H. Gao, M. L. Sh. Gao, Y. Liu, et al., "Determination of Hydroxypolycyclic Aromatic Hydrocarbons in Urine by Electromembrane Extraction Coupled With Liquid Chromatography," *Journal of Chromatography A* 1736 (2024): 465375.

48. B. Pieterse, E. Felzel, R. Winter, B. Van der Burg, and A. Brouwer, "PAH-CALUX, an Optimized Bioassay for AhR-Mediated Hazard Identification of Polycyclic Aromatic Hydrocarbons (PAHs) as Individual Compounds and in Complex Mixtures," *Environmental Science & Technology* 47 (2013): 11651–11659, https://doi.org/10.1021/es403810w.

49. J. Grünfeld, P. Møller, U. Vogel, S. P. Jensen, V. Kofoed-Sørensen, and M.-H. G. Andersen, "Assessment of Polycyclic Aromatic Hydrocarbon Exposure in Trainee Firefighters Using PAH CALUX Bioassay," *Toxics* 12 (2024): 825, https://doi.org/10.3390/toxics12110825.

50. S. Wang, H. Jiang, J. Feng, et al., "Hierarchical Metal-Dielectric-Metal Nanostructures as SERS Sensors for Sensitive Detection of Polycyclic Aromatic Hydrocarbons," *Applied Surface Science* 646 (2024): 158926, https://doi.org/10.1016/j.apsusc.2023.158926.

51. S. Wang, H. Jiang, Y. Jin, et al., "Trace-Level Discrimination and Detection of Polycyclic Aromatic Hydrocarbons via Hybrid Photonic-Plasmonic SERS Sensors Integrated With Machine Learning Algorithms," *Journal of Hazardous Materials* 498 (2025): 140013, https://doi.org/10.1016/j.jhazmat.2025.140013.

52. X. Wang, G. Li, R. Hu, et al., "Chapter 1 - Principles of Surface-Enhanced Raman Spectroscopy," in *Principles and Clinical Diagnostic Applications of Surface-Enhanced Raman Spectroscopy* (Elsevier 2022), 1–32.

53. Z. Xue, X. Zheng, W. Yu, et al., "Review—Research Progress in Detection Technology of Polycyclic Aromatic Hydrocarbons," *Journal of the Electrochemical Society* 168 (2021): 057528, https://doi.org/10.1149/1945-7111/ac0227.

54. X. Wang, Q. Xu, X. Hu, F. Han, and C. Zhu, "Silver-Nanoparticles/Graphene Hybrids for Effective Enrichment and Sensitive SERS Detection of Polycyclic Aromatic Hydrocarbons," *Spectrochimica Acta Part A: Molecular and Biomolecular Spectroscopy* 228 (2020): 117783, https://doi.org/10.1016/j.saa.2019.117783.

55. M.-Y. Wei, S.-D. Wen, X.-Q. Yang, and L.-H. Guo, "Development of Redox-Labeled Electrochemical Immunoassay for Polycyclic Aromatic Hydrocarbons With Controlled Surface Modification and Catalytic Voltammetric Detection," *Biosensors and Bioelectronics* 24 (2009): 2909–2914, https://doi.org/10.1016/j.bios.2009.02.031.

56. L. Ball, H. Carter, C. Baker, and R. Porter, "The Development of Rapid Immunoassays for the Urinary Analysis of 1-Hydroxypyrene Glucuronide Facilitate Both Laboratory and on-Site Polycyclic Aromatic Hydrocarbon Biomonitoring," *Toxicology Letters* 401 (2024): 116–124, https://doi.org/10.1016/j.toxlet.2024.10.002.

57. Y. Fu, C. Chen, X. Li, et al., "Fabrication and Optimization of a Hybrid 3D-Printed Flexible Electrochemical Biosensor for Sensitive Detection of 1-Hydroxypyrene Glucuronide, an Associated Wildfire Exposure Biomarker," *Talanta* 307 (2026): 129778, https://doi.org/10.1016/j.talanta.2026.129778.

58. J. H. Cho, D. Y. Lee, W. K. Lim, and H. J. Shin, "A Recombinant Escherichia Coli Biosensor for Detecting Polycyclic Aromatic Hydrocarbons in Gas and Aqueous Phases," *Preparative Biochemistry and Biotechnology* 44 (2014): 849–860, https://doi.org/10.1080/10826068.2014.887577.

59. O. M. Yaghi, "The Royal Swedish Academy of Sciences has Decided to Award the Nobel Prize in Chemistry 2025 to Susumu Kitagawa (Kyoto

18626319, 2026, 17, Downloaded from https://onlinelibrary.wiley.com/doi/10.1002/pssa.70497 by Martin Konrad - Ku Leuven , Wiley Online Library on [07/09/2026]. See the Terms and Conditions (https://onlinelibrary.wiley.com/terms-and-conditions) on Wiley Online Library for rules of use; OA articles are governed by the applicable Creative Commons License

University, Japan), Richard Robson (University of Melbourne, Australia) and Omar M. Yaghi (University of California, Berkeley, USA) for the Development of Metal-organic Frameworks," accessed March 13, 2026, https://www.nobelprize.org/prizes/chemistry/2025/press-release/.

60. P. Kumar, A. Deep, and K.-H. Kim, "Metal Organic Frameworks for Sensing Applications," *TrAC Trends in Analytical Chemistry* 73 (2015): 39–53, https://doi.org/10.1016/j.trac.2015.04.009.

61. J.-N. Hao and B. Yan, "Determination of Urinary 1-Hydroxypyrene for Biomonitoring of Human Exposure to Polycyclic Aromatic Hydrocarbons Carcinogens by a Lanthanide-Functionalized Metal-Organic Framework Sensor," *Advanced Functional Materials* 27 (2017): 1603856, https://doi.org/10.1002/adfm.v27.6.

62. J. Wang, Z. Yang, W. Chen, et al., "Modulated Light-Activated Electrochemistry at Silicon Functionalized With Metal-Organic Frameworks Towards Addressable DNA Chips," *Biosensors and Bioelectronics* 146 (2019): 111750, https://doi.org/10.1016/j.bios.2019.111750.

63. A. Hernik, M. Sugihara, A. Padunnappattu, N. Stock, R. Ameloot, and I. Naydenova, "Nanoimprinted Holographic MOF Diffraction Gratings - Advancing Selective Volatile Organic Compound Detection at Low Concentrations," *ACS Applied Materials & Interfaces* 17 (2025): 58512–58519, https://doi.org/10.1021/acsami.5c10794.

64. C. Lyu, C. Zhao, M. Wang, et al., "Exactly Restricting the Phenyl Ring Rotation in Metal-Organic Framework for Ultra-Sensitive and Specific Ratiometric Fluorescent Sensing of Sarin," *Aggregate* 6 (2025): e70053, https://doi.org/10.1002/agt2.v6.8.

65. H. Roh, T. J. Quill, G. Chen, et al., "Copper-Based Two-Dimensional Conductive Metal-Organic Framework Thin Films for Ultrasensitive Detection of Perfluoroalkyls in Drinking Water," *ACS Nano* 19 (2025): 6332–6341, https://doi.org/10.1021/acsnano.4c16212.

66. J. Liu, S. Xu, M. Zhang, B. Zhang, Y. Yang, and J. Li, "Exploration of the Capacity of a Superstable Eu-MOF for Visualized Identification of 1 HP and Trp in Fresh Human Urine," *Crystal Growth & Design* 24 (2024): 6472–6482, https://doi.org/10.1021/acs.cgd.4c00764.

67. Y. Wen, J. Liu, J. Pang, J. Li, B. Zhang, and Y. Yang, "Development of a Ratiometric Luminescence Sensor for Convenient Identifying of 1-Hydroxypyrene in Fresh Urine Depended on a CD-Centered MOF," *Crystal Growth & Design* 25 (2025): 6787–6795, https://doi.org/10.1021/acs.cgd.5c00746.

68. Y. Li, Y. Li, Y. Wang, et al., "Application of Zeolitic Imidazolate Frameworks (ZIF-8)/Ionic Liquid Composites Modified Nano-Carbon Paste Electrode as Sensor for Electroanalytical Sensing of 1-Hydroxypyrene," *Microchemical Journal* 159 (2020): 105433, https://doi.org/10.1016/j.microc.2020.105433.

69. Y. Li, Y. Li, C. Du, et al., "Electrochemical Sensing of 1-Hydroxypyrene on a Colloidal Gold Modified Zeolitic Imidazolate Frameworks-67/Carbon Nanofiber Paste Electrode," *Journal of the Electrochemical Society* 168 (2021): 057509, https://doi.org/10.1149/1945-7111/abf216.

70. H. Cui, S. Cui, Q. Tian, et al., "Electrochemical Sensor for the Detection of 1 Hydroxypyrene Based on Composites of PAMAM-Regulated Chromium-Centered Metal-Organic Framework Nanoparticles and Graphene Oxide," *ACS Omega* 6 (2021): 31184–31195, https://doi.org/10.1021/acsomega.1c04765.

71. T. Wu, X.-J. Gao, F. Ge, and H.-G. Zheng, "Metal-Organic Frameworks (MOFs) as Fluorescence Sensors: Principles, Development and Prospects," *CrystEngComm* 24 (2022): 7881, https://doi.org/10.1039/D2CE01159J.

72. O. Vaughan, "Porous by Design," *Nature* 511 (2014): 7509, https://doi.org/10.1038/nature13371.

73. Y. Yang, J. Pang, Y. Li, et al., "Fabrication of a Stable Europium-Based Luminescent Sensor for Fast Detection of Urinary 1 Hydroxypyrene Constructed From a Tetracarboxylate Ligand," *Inorganic Chemistry* 60 (2021): 19189–19196, https://doi.org/10.1021/acs.inorgchem.1c02988.

74. S. Xu, B. Zhang, Y. Li, Y. Yang, J. Li, and J. Pang, "Notably Stable Bifunctional Europium-Centered Metal-Organic Framework for Instant Sensing of Uric Acid and 1 Hydroxypyrene in Human Urine," *Inorganic Chemistry* 62 (2023): 11168–11178, https://doi.org/10.1021/acs.inorgchem.3c01290.

75. S. Xu, J. Pang, B. Zhang, Y. Li, Y. Yang, and J. Li, "Construction of a Sensitive Fluorescence Sensor for Convenient 1 HP and UA Detection Relied on a Stable Eu-MOF," *Crystal Growth & Design* 24 (2024): 1410–1420, https://doi.org/10.1021/acs.cgd.3c01372.

76. J. Zhang, X.-J. Xi, L. Xu, F. Lang, Y. Yang, and J. Pang, "Rare-Earth-Pentacene-Octacarboxylate Frameworks for Highly Efficient Urinary 1-HP Fluorescence Sensing," *Chemical Communications* 61 (2025): 11195, https://doi.org/10.1039/D5CC02537K.

77. S. Xu, J. Liu, B. Zhang, J. Pang, Y. Yang, and J. Li, "Evaluation of the Potential of a Ratiometric Fluorescence Sensor for Sensitively Recognizing 1 Hydroxypyrene in Real Urine Samples Based on a Stable Zn-MOF," *Inorganic Chemistry* 64 (2025): 3969–3978, https://doi.org/10.1021/acs.inorgchem.4c05281.

78. M. Buratti, O. Pellegrino, G. Brambilla, and A. Colombi, "Urinary Excretion of 1-Hydroxypyrene as a Biomarker of Exposure to Polycyclic Aromatic Hydrocarbons From Different Sources," *Biomarkers* 5 (2008): 368–381, https://doi.org/10.1080/135475000424375.

79. J. Lintelmann, X. Wu, E. Kuhn, S. Ritter, C. Schmidt, and R. Zimmermann, "Detection of Monohydroxylated Polycyclic Aromatic Hydrocarbons in Urine and Particulate Matter Using LC Separations Coupled With Integrated SPE and Fluorescence Detection or Coupled With High-Resolution Time-of-Flight Mass Spectrometry," *Biomedical Chromatography* 32 (2018): e4183, https://doi.org/10.1002/bmc.v32.5.

80. Y. Jin, W. Ma, and B. Yan, "Unearth the Luminescence Potential of Metal-Organic Frameworks: Adopting a Feasible Strategy to Fabricate One Ratiometric Fluorescence Sensor for Monitoring Both 1 Hydroxypyrene and Cu^{2+}," *Inorganic Chemistry* 61 (2022): 1349–1359, https://doi.org/10.1021/acs.inorgchem.1c02794.

81. S. Liu, R. Huang, and J. Sun, "Two Isostructural Ln-MOFs With Single Emission Centers: Achieving Ratiometric Fluorescence Sensing of 1-Hydroxypyrene in Human Urine," *Dyes and Pigments* 244 (2026): 113103, https://doi.org/10.1016/j.dyepig.2025.113103.

82. K. C. Honeychurch, J. P. Hart, and N. Kirsch, "Voltammetric, Chromatographic and Mass Spectral Elucidation of the Redox Reactions of 1-Hydroxypyrene Occurring at a Screen-Printed Carbon Electrode," *Electrochimica Acta* 49 (2004): 1141–1149, https://doi.org/10.1016/j.electacta.2003.10.025.

83. Y. Wu, "Determination of 1-Hydroxypyrene in Human Urine by a Multi-Wall Carbon Nanotubes-Modified Glassy Carbon Electrode," *International Journal of Environmental Analytical Chemistry* 91, no. 13 (2011): 1244–1255, https://doi.org/10.1080/03067310903410972.

84. X. Shen, Y. Cui, Y. Pang, and H. Qian, "Pre-Concentration and In Situ Electrochemical Sensing of 1-Hydroxypyrene on an Electrodeposited Poly(3-Methylthiophene) Film Modified Electrode," *Journal of Electroanalytical Chemistry* 667 (2012): 1–6, https://doi.org/10.1016/j.jelechem.2011.12.016.

85. Y. Pang, Y. Huang, W. Li, L. Feng, and X. Shen, "Conjugated Polyelectrolyte/Graphene Multilayer Films for Simultaneous Electrochemical Sensing of Three Monohydroxylated Polycyclic Aromatic Hydrocarbons," *ACS Applied Nano Materials* 2 (2019): 7785–7794, https://doi.org/10.1021/acsanm.9b01821.

86. X.-G. Wang, Q.-S. Wu, and Y.-P. Ding, "Direct Simultaneous Determination of α- and β-Naphthol Isomers at GC-Electrode Modified With CNTs Network Joined by Pt Nanoparticles Through Derivative Voltammetry," *Electroanalysis* 18 (2006): 517–520, https://doi.org/10.1002/elan.v18:5.

18626319, 2026, 17, Downloaded from https://onlinelibrary.wiley.com/doi/10.1002/pssa.70487 by Martin Konrad - Ku Leuven , Wiley Online Library on [07/09/2026]. See the Terms and Conditions (https://onlinelibrary.wiley.com/terms-and-conditions) on Wiley Online Library for rules of use; OA articles are governed by the applicable Creative Commons License

87. J. Muñoz, C. Navarro-Senent, N. Crivillers, and M. Mas-Torrent, "Study of Carbon Nanotube-Rich Impedimetric Recognition Electrode for Ultra-Low Determination of Polycyclic Aromatic Hydrocarbons in Water," *Microchimica Acta* 185 (2018): 255, https://doi.org/10.1007/s00604-018-2783-9.

88. K. S. Novoselov, A. K. Geim, S. V. Morozov, et al., "Electric Field Effect in Atomically Thin Carbon Films," *Science* 306 (2004): 666, https://doi.org/10.1126/science.1102896.

89. J. H. Li, J. Li, H. Feng, et al., "A Facile One-Step In Situ Synthesis of Copper Nanostructures/Graphene Oxide as an Efficient Electrocatalyst for 2-Naphthol Sensing Application," *Electrochimica Acta* 153 (2015): 352–360, https://doi.org/10.1016/j.electacta.2014.11.202.

90. Y.-H. Pang, Y.-Y. Huang, W.-Y. Li, N.-C. Yang, and X.-F. Shen, "Electrochemical Detection of Three Monohydroxylated Polycyclic Aromatic Hydrocarbons Using Electroreduced Graphene Oxide Modified Screen-Printed Electrode," *Electroanalysis* 32 (2020): 1459–1467, https://doi.org/10.1002/elan.v32.7.

91. Z. Pei, L. Li, L. Sun, et al., "Adsorption Characteristics of 1,2,4-Trichlorobenzene, 2,4,6-Trichlorophenol, 2-Naphthol and Naphthalene on Graphene and Graphene Oxide," *Carbon* 51 (2013): 156–163, https://doi.org/10.1016/j.carbon.2012.08.024.

92. M. Cao, A. Fu, Z. Wang, et al., "Electrochemical and Theoretical Study of π-π Stacking Interactions Between Graphitic Surfaces and Pyrene Derivatives," *The Journal of Physical Chemistry C* 118 (2014): 2650–2659, https://doi.org/10.1021/jp411979x.

93. M. Saeki, S. I. Ishiuchi, M. Sakai, and M. Fujii, "Structure of the Jet-Cooled 1-Naphthol Dimer Studied by IR Dip Spectroscopy: Cooperation Between the π-π Interaction and the Hydrogen Bonding," *The Journal of Physical Chemistry A* 111 (2007): 1001–1005, https://doi.org/10.1021/jp0668910.

94. S. Yu, X. Wang, W. Yao, et al., "Macroscopic, Spectroscopic, and Theoretical Investigation for the Interaction of Phenol and Naphthol on Reduced Graphene Oxide," *Environmental Science & Technology* 51 (2017): 3278–3286, https://doi.org/10.1021/acs.est.6b06259.

95. G. Zhao, J. Li, and X. Wang, "Kinetic and Thermodynamic Study of 1-Naphthol Adsorption From Aqueous Solution to Sulfonated Graphene Nanosheets," *Chemical Engineering Journal* 173 (2011): 185–190, https://doi.org/10.1016/j.cej.2011.07.072.

96. V. Georgakilas, M. Otyepka, A. B. Bourlinos, et al., "Functionalization of Graphene: Covalent and Non-Covalent Approaches, Derivatives and Applications," *Chemical Reviews* 112 (2012): 6156–6214, https://doi.org/10.1021/cr3000412.

97. A. Sinha, R. J. Dhanjai, H. Zhao, P. Karolia, and N. Jadon, "Voltammetric Sensing Based on the use of Advanced Carbonaceous Nanomaterials: A Review," *Microchimica Acta* 185 (2018): 89–129, https://doi.org/10.1007/s00604-017-2626-0.

98. X. Shen, Y. Cui, Y. Pang, and H. Qian, "Graphene Oxide Nanoribbon and Polyhedral Oligomeric Silsesquioxane Assembled Composite Frameworks for Pre-Concentrating and Electrochemical Sensing of 1-Hydroxypyrene," *Electrochimica Acta* 59 (2012): 91–99, https://doi.org/10.1016/j.electacta.2011.10.037.

99. Y. Pang, Y. Zhang, W. Li, H. Ding, and X. Shen, "Synergetic Accumulation and Simultaneous Determination of Naphthol Isomers on Electrochemically Reduced Graphene Oxide Modified Electrode," *Journal of Electroanalytical Chemistry* 769 (2016): 89–96, https://doi.org/10.1016/j.jelechem.2016.03.023.

100. L. Gao, Y.-Z. Tang, Y. Hu, G. Zhu, and X. Yang, "Determination of Trace 1-Hydroxypyrene by Resin MN202 With Graphene Composite Modified Glassy Carbon Electrode," *IEEE Sensors Journal* 15, no. 3 (2015): 1475–1481.

101. Y. Pang, Y. Zhang, X. Sun, H. Ding, T. Ma, and X. Shen, "Synergistical Accumulation for Electrochemical Sensing of 1-Hydroxypyrene on Electroreduced Graphene Oxide Electrode," *Talanta* 192 (2019): 387–394, https://doi.org/10.1016/j.talanta.2018.08.042.

102. Y. Pang, N. Yang, X. Shen, Y. Zhang, and L. Feng, "Conjugated Polymer Self-Assembled With Graphene: Synthesis and Electrochemical 1-Hydroxypyrene Sensor," *Polymer* 188 (2020): 122139, https://doi.org/10.1016/j.polymer.2019.122139.

103. G. Zhu, P. Gai, Y. Yang, X. Zhang, and J. Chen, "Electrochemical Sensor for Naphthols Based on Gold Nanoparticles/Hollow Nitrogen-Doped Carbon Microsphere Hybrids Functionalized With SH-β-Cyclodextrin," *Analytica Chimica Acta* 723 (2012): 33, https://doi.org/10.1016/j.aca.2012.02.034.

104. A. Mazzaglia, N. Micali, and L. M. Scolaro, "*Structural Characterization of Colloidal Cyclodextrins: Molecular Recognition by Means of Photophysical Investigation*," in *Cyclodextrin Materials Photochemistry, Photophysics and Photobiology* (Elsevier, 2007).

105. M. A. Casulli, R. Yan, S. Takeuchi, et al., "Cyclodextrin-Based Nanogels for Stabilization and Sensing of Curcumin," *ACS Applied Nano Materials* 7 (2024): 20153–20162, https://doi.org/10.1021/acsanm.4c02972.

106. P. Cui, C. Chen, L. Fang, et al., "Rapid Fabrication of Shaped Cyclodextrin-Based Porous Carbons for Efficient PAHs Capture," *Microporous and Mesoporous Materials* 405 (2026): 114085, https://doi.org/10.1016/j.micromeso.2026.114085.

107. J. Shi, W. Shen, X. Wang, et al., "Simultaneous Detection of Naphthol Isomers With a 3D-Graphene-Nanostructure-Based Electrochemical Microsensor," *Chemosensors* 11 (2023): 217, https://doi.org/10.3390/chemosensors11040217.

108. J. Thangphatthanarungruang, C. Chotsuwan, and W. Siangproh, "A Novel and Easy-to-Construct Polymeric L-Glutamic Acid-Modified Sensor for Urinary 1-Hydroxypyrene Detection: Human Biomonitoring of Polycyclic Aromatic Hydrocarbons Exposure," *Talanta* 253 (2023): 123929, https://doi.org/10.1016/j.talanta.2022.123929.

109. C. Kou, X. Xu, Y. Bao, Z. Guo, and L. Niu, "Liquid-Gated Graphene Field Effect Transistor for High-Performance Label-Free Sensing of Polycyclic Aromatic Hydrocarbons," *Chemosensors* 13 (2025): 56, https://doi.org/10.3390/chemosensors13020056.

110. S. A. Nsibande and P. B. C. Forbes, "Development of a Turn-on Graphene Quantum Dot-Based Fluorescent Probe for Sensing of Pyrene in Water," *RSC Advances* 10 (2020): 12119, https://doi.org/10.1039/C9RA10153E.

111. J. Muñoz, N. Crivillers, and M. Mas-Torrent, "Carbon-Rich Monolayers on ITO as Highly Sensitive Platforms for Detecting Polycyclic Aromatic Hydrocarbons in Water: The Case of Pyrene," *Chemistry – A European Journal* 23 (2017): 15289–15293, https://doi.org/10.1002/chem.v23.61.

112. V. Vivier and M. E. Orazem, "Impedance Analysis of Electrochemical Systems," *Chemical Reviews* 122 (2022): 11131–11168, https://doi.org/10.1021/acs.chemrev.1c00876.

113. J. Muñoz, A. Campos-Lendinez, N. Crivillers, and M. Mas-Torrent, "Selective Discrimination of Toxic Polycyclic Aromatic Hydrocarbons in Water by Targeting π Stacking Interactions," *ACS Applied Materials & Interfaces* 12 (2020): 26688–26693, https://doi.org/10.1021/acsami.0c05557.

114. J. J. BelBruno, "Molecularly Imprinted Polymers," *Chemical Reviews* 119 (2019): 94–119, https://doi.org/10.1021/acs.chemrev.8b00171.

115. J. W. Lowdon, H. Diliën, P. Singla, et al., "MIPs for Commercial Application in Low-Cost Sensors and Assays - An Overview of the Current Status Quo," *Sensors and Actuators B: Chemical* 325 (2020): 128973, https://doi.org/10.1016/j.snb.2020.128973.

116. M. Garg and N. Pamme, "Strategies to Remove Templates From Molecularly Imprinted Polymer (MIP) for Biosensors," *TrAC Trends in Analytical Chemistry* 170 (2024): 117437, https://doi.org/10.1016/j.trac.2023.117437.

117. F. L. Dickert, H. Besenböck, and M. Tortschanoff, "Molecular Imprinting Through Van der Waals Interactions: Fluorescence

18626319, 2026, 17, Downloaded from https://onlinelibrary.wiley.com/doi/10.1002/pssa.70497 by Martin Konrad - Ku Leuven , Wiley Online Library on [07/09/2026]. See the Terms and Conditions (https://onlinelibrary.wiley.com/terms-and-conditions) on Wiley Online Library for rules of use; OA articles are governed by the applicable Creative Commons License

Detection of PAHs in Water," *Advanced Materials* 10 (1998): 149–151, https://doi.org/10.1002/(ISSN)1521-4095.

118. M. Peeters, F. J. Troost, B. van Grinsven, et al., "MIP-Based Biomimetic Sensor for the Electronic Detection of Serotonin in Human Blood Plasma," *Sensors and Actuators B: Chemical* 171-172 (2012): 602, https://doi.org/10.1016/j.snb.2012.05.040.

119. J. Alenus, A. Ethirajan, F. Horemans, et al., "Molecularly Imprinted Polymers as Synthetic Receptors for the QCM-D-Based Detection of L-Nicotine in Diluted Saliva and Urine Samples," *Analytical and Bioanalytical Chemistry* 405 (2013): 6479, https://doi.org/10.1007/s00216-013-7080-1.

120. M. Tertis, P.-L. Sirbu, M. Suciu, et al., "An Innovative Sensor Based on Chitosan and Graphene Oxide for Selective and Highly-Sensitive Detection of Serotonin," *ChemElectroChem* 9 (2022): e202101328, https://doi.org/10.1002/celc.v9.6.

121. M. Serrano, M. Bartolomé, A. Gallego-Picó, R. M. Garcinuño, J. C. Bravo, and P. Fernández, "Synthesis of a Molecularly Imprinted Polymer for the Isolation of 1-Hydroxypyrene in Human Urine," *Talanta* 143 (2015): 71–76, https://doi.org/10.1016/j.talanta.2015.04.092.

122. J. Gonzalez, J. C. Camp, M. Valledor, et al., "Measurement of Polycyclic Aromatic Hydrocarbons by Using Molecularly Imprinted Polymers," in *IEEE International Instrumentation and Measurement Technology Conference, Victoria, Vancouver Island, Canada* (2008).

123. H. Li and L. Wang, "Highly Selective Detection of Polycyclic Aromatic Hydrocarbons Using Multifunctional Magnetic-Luminescent Molecularly Imprinted Polymers," *ACS Applied Materials & Interfaces* 5 (2013): 10502–10509, https://doi.org/10.1021/am4020605.

124. B. D. B. Tiu, R. J. Krupadam, and R. C. Advincula, "Pyrene-Imprinted Polythiophene Sensors for Detection of Polycyclic Aromatic Hydrocarbons," *Sensors and Actuators B: Chemical* 228 (2016): 693–701, https://doi.org/10.1016/j.snb.2016.01.090.

125. U. Latif, L. Ping, and F. L. Dickert, "Conductometric Sensor for PAH Detection With Molecularly Imprinted Polymer as Recognition Layer," *Sensors* 18 (2018): 767, https://doi.org/10.3390/s18030767.

126. O. W. Ngwanya, M. Ward, and P. G. L. Baker, "Molecularly Imprinted Polypyrrole Sensors for the Detection of Pyrene in Aqueous Solutions," *Electrocatalysis* 12 (2021): 165–175, https://doi.org/10.1007/s12678-020-00638-3.

127. E. Mathieu-Scheers, S. Bouden, C. Grillot, et al., "Trace Anthracene Electrochemical Detection Based on Electropolymerized-Molecularly Imprinted Polypyrrole Modified Glassy Carbon Electrode," *Journal of Electroanalytical Chemistry* 848 (2019): 113253, https://doi.org/10.1016/j.jelechem.2019.113253.

128. M. Bartilotti, M. A. Beliomini, and M. V. B. Zanoni, "Using an Electrochemical MIP Sensor for Selective Determination of 1-Naphthol in Oilfield Produced Water," *Electroanalysis* 33, no. 5 (2021): 1346–1355, https://doi.org/10.1002/elan.v33.5.

129. F. Ibrahim, A. Sala, A. Fahs, et al., "Investigation of the Modification of Gold Electrodes by Electrochemical Molecularly Imprinted Polymers as a Selective Layer for the Trace Level Electroanalysis of PAH," *Electrochemistry Communications* 169 (2024): 107837, https://doi.org/10.1016/j.elecom.2024.107837.

130. E. I. Paruli, V. Montagna, M. García-Soto, K. Haupt, and C. Gonzato, "A General Photoiniferter Approach to the Surface Functionalization of Acrylic and Methacrylic Structures Written by Two-Photon Stereolithography," *Nanoscale* 15 (2023): 2860–2870, https://doi.org/10.1039/D2NR06627K.

131. R. W. Hughes, M. E. Lott, R. A. Olson, and B. S. Sumerlin, "Photoiniferter Polymerization: Illuminating the History, Ascendency, and Renaissance," *Progress in Polymer Science* 156 (2024): 101871, https://doi.org/10.1016/j.progpolymsci.2024.101871.

132. D.-H. Yang, C.-S. Lee, B.-H. Jeon, et al., "An Electrochemical Nanofilm Sensor for Determination of 1-Hydroxypyrene Using Molecularly Imprinted Receptors," *Journal of Industrial and Engineering Chemistry (Seoul, Korea)* 51 (2017): 106–112, https://doi.org/10.1016/j.jiec.2017.02.020.

133. X. Li, Y. Huang, M. Chen, Y. Tong, and C. Zhang, "A Label-Free Electrochemical Bisphenol a Immunosensor Based on Chlorogenic Acid as a Redox Probe," *Analytical Methods* 9 (2017): 2183–2188, https://doi.org/10.1039/C6AY02997C.

134. L. A. D. Gugoasa, "Review—Electrochemical Sensors for Determination of the Endocrine Disruptor, Bisphenol A," *Journal of the Electrochemical Society* 167 (2019): 037506, https://doi.org/10.1149/2.0062003JES.

135. C. Wardak, H. Wólczynski, S. Malinowski, B. Paczosa-Bator, and M. Wardak, "A Low-Cost and Environmentally Friendly Electrochemical Biosensor for the Determination of Estradiol," *Materials* 18 (2025): 2932, https://doi.org/10.3390/ma18132932.

136. A. Lalik, J. Szreder, M. Grymel, et al., "Estrogens and Progestogens in Environmental Waters: Analytical Chemistry and Biosensing Perspectives on Methods, Challenges, and Trends," *Analytical Chemistry* 97 (2025): 8654–8683, https://doi.org/10.1021/acs.analchem.4c06796.

137. E.-I. Geana, C. T. Ciucure, A. Soare, S. Enache, E. R. Ionete, and L. A. Dinu, "Electrochemical Detection of Glyphosate in Surface Water Samples Based on Modified Screen-Printed Electrodes," *Nanomaterials* 14 (2024): 948, https://doi.org/10.3390/nano14110948.

138. M. Zhong, H. Zhang, Y. Ren, et al., "Advances in Glyphosate Residue Analysis for Environmental Monitoring: From Chromatography to Immunoassays," *Microchemical Journal* 218 (2025): 115296, https://doi.org/10.1016/j.microc.2025.115296.

139. A. Lalik, J. Szreder, M. Grymel, et al., "Magnetic Ferroferric Oxide and Polydopamine Molecularly Imprinted Polymer Nanocomposites Based Electrochemical Impedance Sensor for the Selective Separation and Sensitive Determination of Dichlorodiphenyltrichloroethane (DDT)," *Analytica Chimica Acta* 10957 (2020): 82–92.

140. F. Caroleo, G. Magna, M. L. Naitana, et al., "Advances in Optical Sensors for Persistent Organic Pollutant Environmental Monitoring," *Sensors* 22 (2022): 2649, https://doi.org/10.3390/s22072649.

141. F. A. Tabar, J. W. Lowdon, S. B. Sichani, et al., "An Overview on Recent Advances in Biomimetic Sensors for the Detection of Perfluoroalkyl Substances," *Sensors* 24 (2024): 1.

142. F. A. Tabar, J. W. Lowdon, M. Frigoli, et al., "Tracking Perfluorooctanoic Acid in Tap and River Water Employing Screen-Printed Electrodes Modified With Molecularly Imprinted Polymers," *ACS Omega* 10 (2025): 15018–15028, https://doi.org/10.1021/acsomega.4c10473.

143. S. Givanoudi, M. Heyndrickx, T. Depuydt, M. Khorshid, J. Robbens, and P. Wagner, "A Review on Bio- and Chemosensors for the Detection of Biogenic Amines in Food Safety Applications: The Status in 2022," *Sensors* 23 (2023): 613, https://doi.org/10.3390/s23020613.

144. W. Yu, Y. Liu, Y. Du, L. Yang, H. Wang, and Y. Huang, "Interpretable Multiwavelength SERS Fingerprints of Human Urine for Ischemic Stroke Diagnosis," *ACS Sensors* 11 (2026): 500–510, https://doi.org/10.1021/acssensors.5c03213.

145. P. Dutta, D. Duleba, A. Martinéz-Aviñó, et al., "Imidacloprid Quantification Directly in Human Urine With Aptamer-Functionalized Nanopipettes," *Electrochimica Acta* 573 (2026): 149433, https://doi.org/10.1016/j.electacta.2026.149433.

146. H. Ren, J. Wang, X. Li, et al., "Eu^{3+} Functionalized Metal-Organic Framework as a Colorimetric and Luminescence Dual-Mode Sensor for Efficient Detection of Carcinoid Tumor Biomarker in Urine," *Journal of Rare Earths*, preprint, December 29, 2025, https://doi.org/10.1016/j.jre.2025.12.025.

147. K. S. Kushwaha, A. Anand, B. Dey, et al., "Novel Electrochemical Sensing Platform Based on Zinc Metal Organic Frameworks/Carbon

18626319, 2026, 17, Downloaded from https://onlinelibrary.wiley.com/doi/10.1002/pssa.70487 by Martin Konrad - Ku Leuven , Wiley Online Library on [07/09/2026]. See the Terms and Conditions (https://onlinelibrary.wiley.com/terms-and-conditions) on Wiley Online Library for rules of use; OA articles are governed by the applicable Creative Commons License

Nanofiber Nanocomposite for Detection of Creatinine in Human Urine," *Journal of Electroanalytical Chemistry* 971 (2024): 118574, https://doi.org/10.1016/j.jelechem.2024.118574.

148. A. Joshi and G. Slaughter, "Electrochemical Carbon-Based Sensors for Non-Enzymatic Uric Acid Sensing," *Microchemical Journal* 208 (2025): 112331, https://doi.org/10.1016/j.microc.2024.112331.

149. M. Caldara, J. W. Lowdon, G. van Wissen, et al., "Dipstick Sensor Based on Molecularly Imprinted Polymer-Coated Screen-Printed Electrodes for the Single-Shot Detection of Glucose in Urine Samples —From Fundamental Study Toward Point-of-Care Application," *Advanced Materials Interfaces* 10 (2023): 2300182, https://doi.org/10.1002/admi.v10.18.

150. S. S. Soliman, A. M. Mahmoud, M. R. Elghobashy, H. E. Zaazaa, and G. A. Sedik, "Point-of-Care Electrochemical Sensor for Selective Determination of Date Rape Drug "Ketamine" Based on Core-Shell Molecularly Imprinted Polymer," *Talanta* 254 (2023): 124151, https://doi.org/10.1016/j.talanta.2022.124151.

18626319, 2026, 17, Downloaded from https://onlinelibrary.wiley.com/doi/10.1002/pssa.70497 by Martin Konrad - Ku Leuven , Wiley Online Library on [07/09/2026]. See the Terms and Conditions (https://onlinelibrary.wiley.com/terms-and-conditions) on Wiley Online Library for rules of use; OA articles are governed by the applicable Creative Commons License

Appendix

TABLE A1 | Alphabetically sorted list of used abbreviations.

Abbreviation	Meaning
3D	Three-dimensional
1OHN	1-Hydroxynaphthalene
1OHP	1-Hydroxypyrene
1OHP-gluc	1-Hydroxypyrene glucuronide
2OHN	2-Hydroxynaphthalene
3OH-Phen	3-Hydroxyphenanthrene
AB	Antibody
Ag	Silver
AG	Antigen
Au	Gold
B[a]P	Benzo[a]pyrene
BSA	Bovine serum albumin
CALUX	Chemical activated luciferase gene expression
Cd	Cadmium
CDs	Cyclodextrins
CNTs	Carbon nanotubes
CPRG	Chlorophenol red-β-galactopyranoside
Cr	Chromium
Cu	Copper
CV	Cyclic voltammetry
DPV	Differential pulse voltammetry
DUV	Deep ultraviolet
E. coli	*Escherichia coli*
EIS	Electrochemical impedance spectroscopy
ELISA	Enzyme-linked immunosorbent assay
Eu	Europium
FD	Fluorescence detection
Fe	Iron
$[Fe(CN)_6]^{3+/4+}$	Ferrocyanide redox complex
FQ	Fluorescence quenching
GC	Gas chromatography
GO	Graphene oxide
GQDs	Graphene quantum dots
HPLC	High-performance liquid chromatography
HRP	Horseradish peroxidase
IgG	Immunoglobulin G
ITO	Indium tin oxide
LOD	Limit of detection
LOQ	Limit of quantification
MIPs	Molecularly imprinted polymers
MOFs	Metal–organic frameworks
MS	Mass spectrometry
MWCNT	Multiwalled carbon nanotubes
OHN	Naphthol
PAHs	Polycyclic aromatic hydrocarbons
PBS	Phosphate-buffered saline
PIL	Polyionic liquid
PMMAYQ	Poly-8-methoxy-7-methyl-5-(10-anthracen-9-yl)quinolone
PPy	Polypyrrole
REACH	Registration, Evaluation, Authorization and Restriction of Chemicals
RGB	Red-green-blue
SAM	Self-assembled monolayer
SERS	Surface-enhanced Raman spectroscopy
SPE	Solid-phase extraction
SWV	Square-wave voltammetry
Tb	Terbium
TiO_2	Titanium dioxide
UV	Ultraviolet
$U_{oxidation}$	Oxidation potential
ZIF	Zeolitic imidazolate framework
Zn	Zinc

18626319, 2026, 17, Downloaded from https://onlinelibrary.wiley.com/doi/10.1002/pssa.70497 by Martin Konrad - Ku Leuven , Wiley Online Library on [07/09/2026]. See the Terms and Conditions (https://onlinelibrary.wiley.com/terms-and-conditions) on Wiley Online Library for rules of use; OA articles are governed by the applicable Creative Commons License